REPORT DOCUMENTATION PAGE

Form Approved OMB No. 0704-0188

1. AGENCY USE ONLY (Leave blank)	2. REPORT DATE	3. REPORT TYPE AND DATES COVERED
	7 July 2000	Final Report

4. TITLE AND SUBTITLE

Testing Of Supersonic COIL Driven By A Jet SOG And Investigation Of Chemical Generation Of Atomic Iodine For COIL

5. FUNDING NUMBERS

F61775-99-WE

6. AUTHOR(S)

Dr. Jarmila Kodymova

7. PERFORMING ORGANIZATION NAME(S) AND ADDRESS(ES)

Institute of Physics Academy of Sciences
Na Slovance 2
Prague 8 182 21
Czech Republic

8. PERFORMING ORGANIZATION REPORT NUMBER

N/A

9. SPONSORING/MONITORING AGENCY NAME(S) AND ADDRESS(ES)

EOARD
PSC 802 BOX 14
FPO 09499-0200

10. SPONSORING/MONITORING AGENCY REPORT NUMBER

SPC 99-4059

11. SUPPLEMENTARY NOTES

2 electronic files.

12a. DISTRIBUTION/AVAILABILITY STATEMENT

Approved for public release; distribution is unlimited.

12b. DISTRIBUTION CODE

A

13. ABSTRACT (Maximum 200 words)

This report results from a contract tasking Institute of Physics, Academy of Sciences as follows: The contractor will investigate the spatial gain and temperature distribution across the gain region of the COIL using a frequency stabilized diode laser as a probe, and the generation of atomic iodine using gaseous compounds.

14. SUBJECT TERMS

EOARD, Chemical lasers, COIL,

15. NUMBER OF PAGES

16. PRICE CODE
N/A

17. SECURITY CLASSIFICATION OF REPORT	18. SECURITY CLASSIFICATION OF THIS PAGE	19. SECURITY CLASSIFICATION OF ABSTRACT	20. LIMITATION OF ABSTRACT
UNCLASSIFIED	UNCLASSIFIED	UNCLASSIFIED	UL

NSN 7540-01-280-5500

Standard Form 298 (Rev. 2-89)
Prescribed by ANSI Std. 239-18
298-102

DEPARTMENT OF THE AIR FORCE

HEADQUARTES, 603D REGIONAL SUPPORT GROUP (USAFE)

European Office of Aerospace Research and Development

(EOARD)

Contract F61775-99-WE059

awarded 7 July 1999

Final Report

addressing all progress on each tasks and conclusion from the investigation

Contract title: **Testing of supersonic COIL driven by a jet SOG and investigation of chemical generation of atomic iodine for COIL**

Principle investigators: **Otomar Špalek, Jarmila Kodymová**

Co-investigators: **Vít Jirásek, Jan Kuželka, Miroslav Čenský**

Contractor: **Jarmila Kodymová**
Department of Gas Lasers
Institute of Physics
Academy of Sciences of the Czech Republic
Na Slovance 2
182 21 Prague 8
Czech Republic
Phone : 420-2-66052699
Fax: 420-2-821227
E-mail: kodym@fzu.cz

Contractor signature:

Date: **7 July, 2000**

Content

1. Testing the supersonic COIL driven by a jet singlet oxygen generator

1.1. Present status of the COIL device

A small-scale 5-cm gain length supersonic COIL of 1 kW class driven by a jet single oxygen generator (jet SOG) with a closed-loop liquid flow system has been developed in the Institute of Physics during the last three years. The main parts of the device and most important parameters are described further.

The jet SOG of rectangular shape (50 x 48 mm of the inner cross section) provides 200 mm high space for a counter flown liquid and gas. A basic hydrogen peroxide (BHP) liquid is injected through the injector made of 6 mm thick plate with 300-380 holes of ∅ 0,8 mm. It corresponds to a jet specific surface area of 3.2 - 4.0 cm^{-1}. The BHP jets are driven by pressure of about 1 atm provided by a gear pump used for BHP loading into the generator room above the liquid injector during BHP circulation. The gear pump (Liquidflo's, Model 312) is equipped with a magnetic coupling and frequency transducer providing the pumping capacity up to 100 litres BHP/min and enables to change the jets velocity from about 6 m/s to 10 m/s. A counter-flown chlorine reacts with perhydroxyl (HO_2^-) ions in the surface layer of 12 cm long BHP jets. Chlorine is delivered into the generator through two injectors formed by stainless steel tube of ∅ 10x1 mm with 23 holes of ∅ 1 mm. The jet SOG is attached directly to a BHP tank. The tank functions also as a mixing tank for BHP preparation from 70 % hydrogen peroxide and 42 % (by weight) potassium hydroxide yielding usually 7 M [HO_2^-].

A water vapour content in gas stream from the generator is controlled by thermal management of the jet SOG with a close-loop flow BHP system including a possible continuous BHP cooling up to –30° C. The cooling enables to reduce the amount of water vapour released during the chlorine-BHP reaction. A cooling power of the heat exchanger (1.4 kW) limits one experimental run to about 4 minutes with 15 litres of BHP and 50 mmol Cl_2/s. The BHP temperature during this operation increases from -25 °C to -8 °C due to BHP/Cl_2 reaction heat of 110.9 kJ/mol.

A primary gas mixture (mostly oxygen + helium) exits the generator through the mechanical choke (the throttle valve, TV) and then passes the electropneumatic flat shut-off valve. A cross section of the opened flat valve copies right the generator exit, i.e. 50 mm by 9.6 mm, together with the diagnostic duct and subsonic channel. The diagnostic duct is equipped with ports for detection of residual chlorine by absorption measurement at 330 nm, the $O_2(^1\Delta_g)$ emission measurement at 1270 nm, and $O_2(^1\Sigma_g)$ emission measurement at 762 nm for water vapor evaluation. EPR spectroscopy was used for calibration of the optical detection method of $O_2(^1\Delta_g)$. Iodine vapor is injected transversely into the primary flow through injectors with two rows of holes on bottom and upper wall of subsonic channel (21 holes of ∅ 0.8 mm and 42 holes of ∅ 0.4, drilled 4 mm downstream). The iodine injectors are resistively heated up to 70 – 90° C. A distance of the I_2 injection plane (the second row of holes) from nozzle throat plane is adjustable from 5 mm to 9 mm.

Iodine vapor is produced from solid iodine stored in a stainless steel tank with capacity enabling the COIL operation with 2 mmol I_2/sec consumption for about 30 min. Iodine can be evaporated partly by outer heating bands, partly by pre-heated helium (up to 500° C) flowing through the iodine bed. The later mainly helps to compensate a heat loss of I_2 bed by iodine evaporation. The 488 nm-absorption of iodine measured in detection cell placed right

downstream of the tank is used for determination of iodine molar flow rate. It is calculated from recorded pressure and temperature in the duct, the secondary helium flow rate and using the absorption cross section $\sigma_{488} = 1.7 \times 10^{-18}$ cm^2. A part of secondary helium by-passes the iodine tank and is added into I_2 + He mixture right before introducing it into the I_2 detection cell. It helps to optimize the penetration of iodine vapours into the primary gas flow.

A single horizontal slit configuration of nozzle is used for the adiabatic expansion of gas flow. The subsonic channel narrows to a nozzle sonic throat of 6.7 mm by 50 mm. The walls of calculated nozzle shape are opened furthermore by 3°. A distance of the sonic plane and resonator optical axis can be adjusted from 35 to 55 mm, the 55 mm distance is used mostly. The 85 cm long resonator in the stable configuration is equipped with mirrors of 5 cm in diameter and 5 m radius of curvature. The mirrors are protected from BHP aerosol and iodine contamination by purging with helium (20 mmol/s). A reflectivity of the back mirror used is 99.95 %, a reflectivity of outcoupling mirrors is in the range of 99.2 % - 97.8 %. The nozzle ramps and mirrors holders limit the multimode output beam size to 3.7 cm in the flow direction by 1.5 cm between the ramps. The 7 % discrete part of total laser power transmitted through the outcoupling mirror was recorded by Labmaster 213 Coherent power meter.

The gas mixture is exhausted from the laser duct through a delta shaped diffuser and liquid nitrogen condenser by the Roots blower with a single-stage rotary pump (Leybold's Ruta 3001) of the total nominal capacity of 3000 m^3/h.

The analogue-digital converter with 32 channels is employed for data acquisition and processing by PC on-line using a software Scopewin modified for the COIL data. The most operations of the whole COIL device are controlled by specially designed computer hardware and developed software.

1.2. Modifications and improvements of the device made recently

- **Modifications of the jet SOG with horizontal gas exit** were introduced and tested in order to suppress BHP droplets escaping into the gas exiting the generator:
  - Inserting two rows of needles of various lengths and arrangement into holes of BHP injector near the generator exit (see **Fig. 1a**),
  - modification of gas outlet from the jet SOG aimed to decrease the velocity of gas crossing the last rows of BHP jets due to enlarging the exit cross-section (see **Fig. 1b**),
  - inserting a special shaped barrier against the liquid creeping along the generator walls (see **Fig. 1c**),
  - inserting droplet separators into the generator exit channel (see **Fig. 1d**),
  - blocking the side holes in the BHP injector aimed to reduce wetting side walls.

- **A new jet SOG with vertical gas exit** was designed and fabricated with the aim to improve the COIL operation by suppressing the BHP droplets escaping from the generator. A design of this generator was adapted to other existing parts of the COIL device. The technical drawing of this generator was enclosed to the Report 0002 of this Contract, the principle can be seen in **Fig. 2**. The gas generated by g/l reaction in the reactor (1) exits through metal tubes (2) (either 8 tubes of ∅ 8/6 mm or 4 tubes ∅ 10/8 mm) fixed between the BHP injector plate (3) and the plate (4) dividing BHP liquid cavity (5) and the upper gas cavity (6). This gas outlet arrangement is advantageous in (i) a larger cross-section of gas stream crossing the jets comparing to the former jet SOG, and (ii) in droplets separation from the

exiting gas by a sudden change in gas flow direction. An additional volume (the room in the upper gas cavity) in which some loss of singlet oxygen occurred was reduced later by a filler (not shown in the figure). A testing the COIL operation with the "vertical" generator started about a month ago.

- **Improvements of iodine management** consists in a more explicit control of gas flow rates in iodine system. In our COIL, flow of secondary helium is divided into two streams (one part of He flows through the I_2 tank, second part by-passes the tank). In the former arrangement, the overall He_{sec} flow rate was measured only. In the new arrangement, flowrate of both streams are measured independently and recorded on-line.

- **Further laser parameters included into the automatic data evaluation** :
  - instantaneous values of iodine flow rate,
  - flow rates of He_{sec} through the iodine tank and He_{sec} by-passing the tank (in addition to flow rates of all primary gases),
  - the secondary gas mixing ratio, i.e. n_{He}/n_{I2},
  - the calculated singlet oxygen yield, Y_Δ, in conditions when iodine is injected into the primary flow and interfering 1.315 μm with 1.27 nm signal (see **Fig. 3**); the calculated yield represents the average Y_Δ value obtained from measurements without iodine in the same other flow conditions,
  - the relative penetration factor, Π, i.e., the ratio of penetration parameter, π, to the full penetration parameter, π_{full}, defined as[1]

$$\pi = (n_s/n_p)\,(M_s T_s P_p/M_p T_p P_s)^{1/2} \qquad (1\text{-}1)$$

where indexes *p* and *s* represent the properties of primary and secondary gas flow (n - molar flow rate, T - temperature, P - pressure, and M - molecular weight). The π_{full} parameter representing the full penetration of secondary flow into the primary flow is evaluated from the device hardware data by

$$\pi_{full} = (d\,A_s)/(5DA_p) \qquad (1\text{-}2)$$

where d is the height of primary flow channel, A is the flow cross-section of gas channel (*p*) and overall I_2 injector holes (*s*), and D is the diameter of injector holes.

  - the instantaneous cross-section of I_2 injector holes enabling to recognize a blocking of iodine injector holes by solid iodine or BHP during experiment; evaluated from the equation valid for the gas mass flow rate, G, in sonic conditions[2]

$$G = C\,S\{P_1^2\,M\,[2/(\kappa+1)]^{(\kappa+1)/(\kappa-1)}\}^{0.5} \qquad (1\text{-}3)$$

where C is the constant dependent on holes shape, S is the overall holes cross-section, P_1 is pressure before the holes, M is the molecular weight and κ is the adiabatic constant of the gas mixture (I_2+He_{sec}).

- **System of automatic controlling the COIL operation** was designed and a special hardware and software was developed. It enables to control the function of most valves: opening and shutting of the valve for Cl_2 flow, He_{prim} flow, the flat gate valve at the

generator exit, valves closing tubes by-passing the laser and iodine injector. The system controls the operation of the throttle valve (a proportional one) (TV – see Fig. 1) for adjusting a needed pressure in the generator, proportional valves for secondary He flow through the I_2 tank and by-passing the tank and adjusting so a required I_2 flow rate. These two valves enable also to maintain the total He_{sec} flow rate on needed level.
In addition to a more reliable control of the COIL operation and possible much faster sequence of individual operations, this automation increases the device security against dangerous situations in the case of some breakdown.

1.3. Testing the COIL device

1.3.1. Jet SOG operation

Many experimental runs were performed to test the jet SOG of both types, i.e. with either horizontal or vertical gas exit along with the laser operation. The reason for this investigation was to optimize the generator parameters mostly from the point of minimization of BHP droplets escaping into the gas flowing into the cavity.

Pressure conditions in the jet SOG and so a singlet oxygen yield are controlled easily by the valve throttling at the generator exit. Examples of dependence of the yield on generator pressure for jet SOG with horizontal gas exit are illustrated in Figs. 1, 4 and 5 presented in the Report 0002 of this Contract. A considerable increase in the yield with the pressure decrease results from a shorter gas residence time in the generator and lower $O_2(^1\Delta_g)$ partial pressure. Both effects reduce the $O_2(^1\Delta_g)$ loss by self-quenching reactions (the pooling and dimolar reaction)

$$O_2(^1\Delta_g) + O_2(^1\Delta_g) \rightarrow O_2(^3\Sigma_g) + O_2(^1\Sigma_g) \qquad k_4 = 2.7\text{x}10^{-17}\ \text{cm}^3\ \text{s}^{-1} \qquad (1\text{-}4)$$

$$O_2(^1\Delta_g) + O_2(^1\Delta_g) \rightarrow 2\ O_2(^3\Sigma_g) \qquad k_5 = 1.7\text{x}10^{-17}\ \text{cm}^3\ \text{s}^{-1} \qquad (1\text{-}5)$$

The jet SOG with vertical gas exit provided rather high $O_2(^1\Delta_g)$ yields that were still increased by about 5 % in the case when the gas space in the upper part of generator body was n the first version of, were by lower due to the additional (see Fig. 2). When this space was substantially reduced by insertion a filler in the form of two prisms. The $O_2(^1\Delta_g)$ yield, Y_Δ, measured for several values of generator pressure is documented in **Tab. 1** and **Fig. 4**.

Tab. 1

P_G, kPa (Torr)	3 (22.5)	5 (37.5)	8 (60)	10 (75)	12 (90)	15 (112.5)
Y_Δ, %	80	74	65	58	52	43

It was verified that liquid droplets escaping from the modified generator is suppressed due to a higher cross section (and consequently lower gas velocity) in which exiting gas crosses BHP jets. Further improvement of the jet SOG operation was achieved by enlarging (by drilling) the upper part of holes in the jet injector from 0.8 mm to 1.2 mm which resulted

in a pressure loss reduction along the BHP injector plate. In this way, the BHP re-pumping rate together with the jet velocity could be increased (from 6 m/s to 9 m/s) and so also the jets stability.

Another unfavourable effect of the closed loop system with BHP re-pumping is created by a BHP liquid over-saturation with oxygen and circulation of small gas bubbles. In the moment when BHP liquid leaves the jet injector, the pressure drops and the size of oxygen bubbles grows dramatically causing the jets breaking. A great amount of BHP droplets is so formed and some of them are carried with gas into the gas channel and cavity. It is the most probable and the reason for a time decrease in laser power often observed, which is caused by light scattering on flying BHP droplets.

A cooling power of 1.4 kW of the heat exchanger employed was not sufficient to balance the BHP heating by reaction heat of 110.9 kJ/mol released in the process

$$Cl_2 + HO_2^- + OH^- \rightarrow O_2(^1\Delta_g) + H_2O + 2\,Cl^- \qquad (1\text{-}6)$$

and the exothermic reactions (1-4) and (1-5). For this reason, one experimental run was limited for a few minutes only to avoid a power drop or power killing by water vapor. A time course of typical BHP temperature increase was presented in Fig. 3 of the Report 0002 of this Contract.

1. 3.2. Gas dynamic conditions in COIL system

Gas dynamic conditions in the subsonic channel and supersonic region of laser device were tested during a „cold flow run", i.e. gaseous nitrogen was used instead of chlorine and no iodine was injected into the primary flow. The average Mach number, M_1, for a subsonic flow upstream of the sonic throat, and for the supersonic flow in the resonator region, M_2, were evaluated from pressure measurements in the respective region, gas flow rates (n), physical properties of the flowing gas (molecular weight, Mw, adiabatic constant, κ), stagnation temperature, and flow cross section, A.[3] Typical values of the average Mach numbers are in **Tabs. 2** and **3**.

Tab. 2

P_1, Pa	n_{N2}, mmol/s	n_{He}, mmol/s	Mw, kg/mol	κ	**M_1**
2055	22.3	89.5	8.79×10^{-3}	1.58	**0.41**

Tab. 3

P_2, Pa	n_{N2}, mmol/s	n_{He}, mmol/s	Mw, kg/mol	κ	**M_2**
174	20.5	91.4	8.37×10^{-3}	1.57	**1.94**

The local Mach number, M_2', in the supersonic region was evaluated from the pressure ratio P_{stat}/P_{Pit}, where P_{stat} is the static pressure measured near the cavity wall, and P_{Pit} is the stagnation pressure measured by the Pitot tube in the cavity centreline.[4] In **Tab. 4**, the M_2'

value calculated for given experimental conditions and A = 9.16×10^{-4} m^2 corresponds to the Pitot tube position at a distance of 55 mm from the sonic throat plane where the cavity is 16 mm high and 55 mm wide.

Tab. 4

P_{stat}, Pa	P_{Pit}, Pa	n_{N2}, mmol/s	n_{He}, mmol/s	κ	M_2'
174	1457	20.5	91.4	1.57	**2.37**

1.3.3. Laser operation as a whole

a) Laser driven by jet SOG with horizontal gas exit

A substantial effect of iodine flow rate on the laser power is illustrated in **Fig. 5** showing a simultaneous time courses of both parameters during one experimental run. The I_2 flow rate was controlled by the ratio of secondary helium flowing through the iodine tank and by-passing it. The measurement was performed at 40 mmol Cl_2/s, 80 mmol He_{prim}/s, 40 mmol He_{sec}/s, and the outcoupling mirror transmittance of 2.83 %. This figure shows that laser power of 400 ± 25 W was reproducible in the optimum range of 1.0 - 1.75 mmol I_2/s, i.e., $[I_2]/[O_2] = 0.025 \div 0.043$. A relative shortage of I_2 in the system against $O_2(^1\Delta_g)$ slows down dissociation process, which limits both the gain and power. An excess of I_2 in the laser medium has a quenching effect on excited atomic iodine in the fast reaction

$$I(^2P_{1/2}) + I_2 \rightarrow I(^2P_{3/2}) + I_2 \qquad k_7 = 3.5 \times 10^{-11}\ cm^3\ s^{-1} \qquad (1\text{-}7)$$

The data from these measurements were used to plot the dependence of laser power as a function of iodine flow rate (see **Fig. 6**). Similar plots were obtained also for several other transmittances of outcoupling mirror (see **Fig. 7**). These experimental data made possible to evaluate the gain and saturation intensity (see **Tab. 5**).

Tab. 5

n_{I2}, mmol s^{-1}	$\alpha_{34} \times 10^{-2}$, cm^{-1}	I_s, kW/cm^2
0.50	1.23	7.1
0.75	1.27	6.5
1.00	1.29	5.8
1.25	1.30	5.3
1.50	1.29	5.4
1.75	1.28	4.7

An effect of the titration ratio, i.e. $[I_2]/[O_2(^1\Delta_g)]$, on the laser power was investigated for different outcoupling mirror reflectivity. A set of this dependence shows a maximum for the titration ratio between 5 to 8 %. According to these results, the highest power was mostly achieved for $[I_2]/[O_2(^1\Delta_g)]$ = (5±1) % (outcoupling δ_e = 2.88 %). An example of this

dependence is illustrated in **Fig. 8** for two values of generator pressure. It was shown that a higher pressure in the jet SOG (resulting in a lower $O_2(^1\Delta_g)$ yield) was reflected in a lower laser power in the whole tested region. A similar value of the titration ratio was obtained for the maximum power with the outcoupling of 2.85 % on the 10 kW COIL device in DLR Institute.[5] The maximum power on the VertiCOIL system at AFRL was obtained for I_2/O_2 ratio of about 1.7 only.[6] However, dividing this value by the $O_2(^1\Delta_g)$ yield of 0.54 estimated by the authors results in the optimum $I_2/O_2(^1\Delta_g)$ ratio of 3.1 % which is closer to our result.

An effect of generator pressure on the laser power was studied also for pressures below 8 kPa (for 40 mmol Cl_2/s and 80 mmol He_{prim}/s). It was expected that the power would increase with decreasing the generator pressure due to increasing $O_2(^1\Delta_g)$ yield (for the optimal $I_2/O_2(^1\Delta_g)$ ratio). The results obtained in many experimental tests, however, showed, that this presumption is not valid (for pressures less than 8 kPa, and the He_{prim}/Cl_2 ratio about 2). It is obvious from **Fig. 9**. The power drop connected with the generator pressure decrease from 8.8 to 4.9 kPa (due to the throttle valve opening from position 4 to 9) was most probably caused by laser energy loss due to a light scattering on liquid droplets, the amount of which increased with decreasing generator pressure and resulting in increasing gas flow velocity. With a lesser gas flow throttling, flying droplets were visualized by illumination in the laser cavity, and their settling in the form of solid layer on the walls of channel and supersonic nozzle throat. As the water vapor content evaluated from detection in subsonic channel increased only slightly in the case of more opened throttle valve (TV) (**Tab. 6**) but the laser power drop was substantial (see **Fig. 9**), it is supposed that BHP droplets are not evaporated mostly in the subsonic part of the device and fly as far as to the cavity.

Tab. 6

TV position	4	9
P_{gen}, kPa (Torr)	7.4 (55.5)	5,0 (37.5)
P_{H2O}, Pa (Torr)	39 (0.3)	50 (0.4)
P_{H2O}/P_{Δ}, %	5.7	7.4

An effect of the dilution ratio, $[He_{sec}]/[I_2]$, on laser power was investigated in other experimental sets for several values of outcoupling mirror reflectivity. It was found that this dependence has a maximum at dilutions in the range from 1:30 to 1:70 (see e.g. **Fig. 10**). A decline of the power at lower iodine dilution can be ascribed to deteriorated mixing of primary and secondary gas. It is caused by a formation of regions with high local concentration of molecular iodine where $O_2(^1\Delta)$ is consumed mostly in I_2 dissociation.

The effect of penetration of secondary gas flow (I_2+He_{sec}) into the primary gas flow ($O_2(^1\Delta_g)$+He_{prim}) on laser power is shown in **Fig. 11.** The evaluated π_{full} parameter equals to about 0.11. Plots of power on the relative penetration factor Π_{rel} given by the ratio π/π_{full} show mostly a flat maximum in the range of 0.8 to 1.0. It corresponds with theoretical assumptions[1,6] of optimum mixing of primary and secondary flows, i.e. the secondary gas penetrates entirely into the primary gas flow and formation of boundary layers or central zone with high I_2 concentration is suppressed.

b) Laser driven by jet SOG with vertical gas exit

A few experimental series testing the COIL with "vertical" jet SOG were performed up to now. An example of the time course of several parameters is plotted in **Figs. 12.** The **Fig. 12a** shows an example of plot of the laser power as a function of changing iodine flow rate in the range of 1.25 to 2.2 mmol/s during one experimental run lasting ~ 90 seconds. The relative penetration factor evaluated for a variable dilution ratio (the ratio of He_{sec} flow rate to I_2 flow rate) is also shown in this figure and approached the optimum value 1 for the dilution ratio of around 20. The Cl_2 flow rate of 40 mmol/s, and He_{prim} flow rate of 80 mmol/s was kept constant during the entire experimental run.

It was observed that the BHP droplets escaping into the gas channel and their settling on the walls can cause a blocking (partly or fully) the holes of I_2 injector placed at the bottom and upper channel walls. A similar holes blocking could be caused by iodine when the I_2 flow rate is too high. The I_2 concentration evaluated in the detection cell upstream the injector do not correspond then to a real I_2 flowing into the laser if the injector holes are partly blocked. The holes blocking was therefore inspected continuously during the experimental run by evaluating their free cross-section. A value of the cross-section calculated from number and size of the holes was compared with a value calculated by the hydrodynamic eq. (1-3). It is documented in **Fig. 12b**. It can be seen that on the increase I_2 flow rate up to 2.25 mmol/s, a reduction of free cross-section followed which was reflected also in a pressure increase in the iodine injector.

1. 3.4. Status quo of performance characteristics of the COIL device

Summary of the performance characteristics corresponding to the most favourable COIL operation so far is in **Tab. 7.**

Tab. 7

Laser power	430 W
Running time	1.5 min
Chlorine flowrate	37.8 mmol/s
Primary helium diluent	80 mmol/s
Generator pressure	8 kPa (60 Torr)
Chlorine utilization	0.97
Starting BHP molarity	6.7 M HO_2^-
$O_2(^1\Delta_g)$ measured yield	0.72
Subsonic channel temperature	+2°C
Subsonic channel pressure	3.8 kPa (28.5 Torr)
Laser cavity pressure	380 Pa (2.8 Torr)
I_2 /O_2 flow rate ratio	0.029
Penetration parameter, π	0.093
Full penetration parameter, π_{full}	0.105
Mirrors reflectivity	0.9995/0.981
Mode length	3.7 cm
Small signal gain	0.015 cm^{-1}
Saturation intensity	4 kW/cm^2
Chemical efficiency	0.12

1.4. Summary of results and conclusion from the investigation

Testing the jet SOG with BHP re-circulation and horizontal gas exit

- High yields of $O_2(^1\Delta_g)$ with a low content of water vapor were attained.
- The $O_2(^1\Delta_g)$ generation was accompanied with a great amount of BHP droplets entrained into the gas channel and laser cavity.
- Constructional modifications of the generator exit aimed to suppress liquid droplet escaping were successful only partially.

Design and development of jet SOG with vertical gas exit

- The first tests were performed and preliminary results were obtained.
- $O_2(^1\Delta_g)$ yields are comparable to yields from the "horizontal-version" SOG in similar conditions.
- Amount of BHP droplets in exiting gas was reduced but not fully avoided yet.

Iodine management

- Controlling the secondary helium flow through the iodine tank and by-passing the tank was introduced allowing and a substantially control of I_2 flow into the laser.

Data acquisition system

- A number of automatically evaluated data was extended by other parameters like the secondary mixing ratio, the n_{He}/n_{I2}, titration ratio, the $n_{I2}/n_{O2(\Delta)}$, relative penetration parameter, and instantaneous cross-section of iodine injector holes (from a monitoring of injector holes blocking by solid I_2 or BHP film).

Automatic control of the COIL operation

- A controlling system including special hardware and software was developed enabling to control:
  - opening and closing nearly all valves of the system in needed consequence,
  - generator pressure by adjusting the throttle valve position at generator exit,
  - iodine flow rate according to measured iodine concentration by adjusting the ratio of secondary helium flow rates through I_2 tank a by-passing the tank,
  - secondary helium flow rate by means of two proportional valves.

Tests of COIL operation

- The effect of generator pressure on laser power was determined and explained.
- Effects of iodine flow rate and mirrors outcoupling on laser power were found, interpreted, and used for estimating the small signal gain and saturation intensity.
- The effect of titration ratio $[I_2]/[O_2]$ on laser power was found and interpreted. Its optimal value of 3.4 ± 0.7 %, and $[I_2]/[O_2(\Delta)] = 5 \pm 1$ % was determined (at optimal outcoupling of 2.88 %), respective values were found also for other mirror outcoupling.
- The effect of iodine dilution ratio $[He_{sec}]/[I_2]$ on laser power was found and interpreted. The optimal value ranges from 30 to 70.

The performance characteristics corresponding to the most favourable COIL operation of our COIL device are not optimal yet. It is documented for instance by relatively low chemical efficiency of the device (12.5 %). The main reasons for this fact follow from a decisive impact on laser power by liquid droplets escaping from the jet SOG (including a time effect due to over-saturation of BHP by produced oxygen during BHP re-circulation), and the quality of resonator mirrors. Solving these tasks remains for our next work.

2. Investigation of chemical generation of I atoms for a COIL

A suggested chemical procedure of I atoms generation directly in the COIL medium is aimed to a) avoid disadvantages of using molecular iodine as I source in conventional COIL operation that reduce the extractable energy of $O_2(^1\Delta_g)$ by loss in I_2 dissociation (remaining still the unresolved process of COIL kinetics) and also quenches excited I atoms. Using solid or liquid I_2 brings also some technical inconveniences with I_2 evaporation and I_2 vapor transport which necessitates a sophisticated management. b) use gaseous reactants only from commercially available gases; c) develop an alternative method of I atoms production by I_2 dissociation using electric discharge techniques or photolysis of alkyliodides.

2.1. Methodology

2.1.1. Suggestion of reaction scheme

Following from the literature review presented in the Report 0001 of this Contract, the suggested **principal process for I atom generation** is based on the fast reaction between halogen atoms and hydrogen iodide molecules

$$X + HI \rightarrow HX\ (HX^*) + \mathbf{I(^2P_{3/2})}$$

with X = F or Cl.

Purely chemical generation of halogen atoms is the first step in the multiple chemical processes.

Generation of F atoms: F atoms can be generated by the fast temperature dependent reaction of nitric oxide with molecular fluorine

$$NO + F_2 \rightarrow NOF\ (NOF^*) + \mathbf{F} \qquad k_1 = 7 \times 10^{-13}\, e^{-1150/T}\ cm^3s^{-1} \qquad (2\text{-}1)$$

This exothermic reaction by 77 kJ/mol is accompanied by loss processes. Some important are

$$F + NO + NO \rightarrow NOF + NO \qquad k_2 = 1.7 \times 10^{-31}\ cm^6s^{-1} \qquad (2\text{-}2)$$

$$F + NO + He \rightarrow NOF + He \qquad k_3 = 1.1 \times 10^{-31}\ cm^6s^{-1} \qquad (2\text{-}3)$$

$$F + wall \rightarrow products \qquad k_4 = 12 \pm 19\ s^{-1} \qquad (2\text{-}4)$$

$$F + F + M\ (He) \rightarrow F_2 + M \qquad k_5 = 5.3 \times 10^{-34} \qquad (2\text{-}5)$$

Generation of Cl atoms: Cl atoms can be generated by the fast exothermic (97.8 kJ/mol) reaction of nitric oxide with chlorine dioxide

$$2NO + ClO_2 \rightarrow 2NO_2 + \mathbf{Cl} \qquad (2\text{-}6)$$

running by branched chain reaction scheme

$$NO + ClO_2 \rightarrow NO_2 + ClO + 60.6\ kJ/mol \qquad k_7 = 3.4\times10^{-13}\ cm^3s^{-1} \qquad (2\text{-}7)$$

$$ClO + NO \rightarrow NO_2 + Cl + 37.2\ kJ/mol \qquad k_8 = 1.7\times10^{-11}e^{(120/T)}\ cm^3s^{-1} \qquad (2\text{-}8)$$

$$Cl + ClO_2 \rightarrow 2\ ClO + 23.4\ kJ/mol \qquad k_9 = 5.9\times10^{-11}cm^3s^{-1} \qquad (2\text{-}9)$$

The reaction (7) initiates the chain while reaction (8) and (9) propagate the chain with Cl and ClO radical acting as chain carriers. With the initial NO concentration twice of ClO_2, the Cl atoms are produced according to the reaction (6). For efficient use of NO/ClO_2 reaction scheme, the chain carriers Cl and ClO must not be excessively depleted by loss processes. The most important loss process for both Cl and ClO is the termolecular reaction with NO_2, an unavoidable stable product of the branched chain process (reactions (7) and (8))

$$Cl + NO_2 + He \rightarrow ClNO_2 + He \qquad k_{10} = 7.2\times10^{-31}cm^6s^{-1} \qquad (2\text{-}10)$$

$$ClNO_2 + Cl \rightarrow Cl_2 + NO_2 \qquad k_{11} = 3.0\times10^{-11}cm^3s^{-1} \qquad (2\text{-}11)$$

$$ClO + NO_2 + He \rightarrow NO_3Cl + He \qquad k_{12} = 1.0\times10^{-31}cm^6s^{-1} \qquad (2\text{-}12)$$

The recombination reaction of Cl atoms is by two orders slower

$$Cl + Cl + M \rightarrow Cl_2 + M \qquad k_{13} = 6.4\times10^{-33}cm^6s^{-1} \qquad (2\text{-}13)$$

The necessary gaseous ClO_2 for the reaction with NO can be produced by in laboratory available procedure - the heterogeneous reaction between solid sodium chlorite ($NaClO_2$) and gaseous chlorine

$$2NaClO_2(s) + Cl_2(g) \rightarrow 2ClO_2 + 2NaCl \qquad (2\text{-}14)$$

Generation of I atoms: I atoms generation is the second step in the multiple gas phase chemical processes and is realized by injection of HI into the medium with F or Cl atoms. It goes though very exothermic reactions (15) and (16), and besides atomic iodine, vibrationally excited HF or HCl (up to 70 %) are produced

$$F + HI \rightarrow HF\ (HF^*) + \mathbf{I(^2P_{3/2})} + 216.7\ kJ/mol \qquad k_{15} = 7.3\times10^{-12}\ cm^3s^{-1} \qquad (2\text{-}15)$$

$$Cl + HI \rightarrow HCl\ (HCl^*) + \mathbf{I(^2P_{3/2})} + 132.5\ kJ/mol \qquad k_{16} = 1.64\times10^{-10}cm^3s^{-1} \qquad (2\text{-}16)$$

Pumping reaction: The energy transfer reaction between generated I atoms and $O_2(^1\Delta_g)$ contained in the primary flow and generating the excited I atoms, $I(^2P_{1/2})$, is the third step in the whole reaction kinetics

$$I(^2P_{3/2}) + O_2(^1\Delta_g) \rightarrow \mathbf{I(^2P_{1/2})} + O_2(^3\Sigma_g) \qquad k_{17} = 7.6\times10^{-11}\ cm^3s^{-1} \qquad (2\text{-}17)$$

An effective chemical generation of I atoms assumes a slow quenching of $O_2(^1\Delta_g)$ and I^* by reactants, reaction intermediates and reaction products. It follows from the literature review, that the reaction between $O_2(^1\Delta_g)$ and HI, HCl or NO can be neglected in comparison with the rate of the pumping reaction (2-17)

$$O_2(^1\Delta_g) + HI \rightarrow O_2(^3\Sigma_g) + HI^{(*)} \qquad k_{18} \leq 2\text{x}10^{-17}\ cm^3s^{-1} \qquad (2\text{-}18)$$
$$O_2(^1\Delta_g) + HCl \rightarrow O_2(^3\Sigma_g) + HCl^{(*)} \qquad k_{19} = 4\text{x}10^{-18}\ cm^3s^{-1} \qquad (2\text{-}19)$$
$$O_2(^1\Delta_g) + NO \rightarrow O_2(^3\Sigma_g) + NO \qquad k_{20} = (5\pm1)\text{x}10^{-17} cm^3s^{-1} \qquad (2\text{-}20)$$

Also I^* quenching by HI or HCl are relatively slow reactions

$$HI + I^* \rightarrow HI + I \qquad k_{21} = 5.7\text{x}10^{-14}\ cm^3s^{-1} \qquad (2\text{-}21)$$
$$HCl + I^* \rightarrow HCl + I \qquad k_{22} = 1.4\text{x}10^{-14}\ cm^3s^{-1} \qquad (2\text{-}22)$$

A quenching of $O_2(^1\Delta_g)$ or I^* can be caused by ClO_2, NO_2Cl or NO_3Cl present in the reaction system, however, the rate constants for these processes were not found.

2.1.2. Modeling of reaction systems

A model based on the generalized one-dimensional (1-D) flow development of chemical processes during I atoms generation by both above reaction schemes (i.e., via F and Cl atoms, respectively) was formulated for the flow conditions characteristic for a subsonic gas region of the COIL device in the Institute of Physics (a total pressure of 4 kPa (30 Torr) corresponding to the flow rates of 40 mmol Cl_2/s, 80 mmol He_{prim}/s, 40 mmol He_{sec}/s, 1.1 mmol I_2/s, and gas flow velocity of 100 m/s). The 1-D model describes the flow of reactants assuming their instantaneous mixing with neglecting the heat transfer to walls. The model includes also the enthalpy balance with $c_p \neq f(T)$.

The results of modeling of chemical generation of I atoms via F atoms (i.e., reactions (1)-(5) and (15)) showed that in optimum conditions nearly 90 % conversion of HI into I atom can be obtained, however, the reaction path is very long (50 cm), and residual NO in the system is very high (about 50 %). The results of modeling of I atoms generation via Cl atoms (reactions (6)-(12) and (16)) showed that up to 90 % conversion of HI to I can be expected on 10 cm reaction path with more than 90 % conversion of NO and ClO_2. **Fig. 13** shows such results for the case when HI is injected together with (ClO_2+NO+He) mixture ([ClO_2]:[NO]:[He]:[HI] = 1:2:75:1). It can be seen that more then 80 % yield of I is attained on 5 cm distance from the injection point. In **Fig. 14**, the HI is injected about 0.5 cm downstream of the(ClO_2+NO+He) mixture injection corresponding to the maximum concentration of Cl atoms in the reaction system. In this case, the 78 % conversion of HI to I atoms is attainable on only 3 cm flow path.

Proceeding from the results of modeling that were described in more detail in the interim Report 0001 of the Contract F61775-99-WE059 delivered to the EOARD, our further study of chemical generation of I atoms for a COIL has been focused on the reaction system via Cl atoms.

2.1.3. Design and development of small-scale experimental device

A small-scale device was designed for the experimental conditions simulating the flow and pressure conditions in the subsonic flow of COIL in the Institute of Physics. Supposed that an instantaneous ideal mixing of reactants occurs, conclusions from the modeling may be used for any inert gas used as diluent, and therefore the apparatus was designed for using nitrogen instead of helium because of cost.

The device is shown schematically in **Fig. 15.** A flow chemical reactor 1 is made of stainless steel tube of 10 mm in inner diameter. It is equipped with three injectors (I #1-3) made of stainless steel tubes of outer diameter of 5 mm with drilled holes at the ends. A diameter and number of the holes in each injector resulted from calculations based on fulfilling the condition of full penetration of secondary gas injected into the primary gas. Further, the pressure in each injector, as well as before the measuring diaphragm of flowmeters (6-8 in Fig.15) corresponds to a sonic speed in holes. The injector # 1 has 24 holes of ∅ 0.4 mm, the injector # 2 has 20 holes of ∅ 0.4 mm, and the injector # 3 has 16 holes of ∅ 0.4 mm. The injectors are places in bends of the reactor, inserted coaxially in the reactor tube, and a distance among the three injection points inside the reactor can be adjusted by moving injectors. In this way, a time delay between injection of individual secondary gases can be varied achieving so the effective reactants mixing.

A mixture of ClO_2+N_2 (1:50) is introduced into the reactor as a primary gas. The first half amount of NO+N_2 (1:10) mixture is injected by the injector # 1 as the first secondary gas. A flow rate of this mixture is controlled by a stainless steel needle valve, measured by flowmeter 6, and evaluated from pressure measured before a diaphragm orifice of the flowmeter. The second half amount of NO+N_2 mixture is injected by the injector # 2 as the second secondary gas measured by the flowmeter 7. The reason for injecting the NO+N_2 mixture step by step follows from the reaction kinetics of Cl atoms production. A more stable radical ClO than Cl atom is produced in the first step of the branched chain process. The rate of loss reaction of ClO with NO_2 (reaction by-product) (eq. (2-12)) is seven times slower than the rate of analogue loss reaction of Cl (eq. (2-10)). It is also the reason for as short as possible distance between injectors # 2 an #3 (supposing instantaneous mixing). Hydrogen iodide (HI) diluted with nitrogen (1:10) is injected by the injector # 3 as the third secondary gas on a distance adjusted as short as possible in order to minimize a loss of produced Cl atoms. A flow rate the HI+N_2 mixture is controlled by needle valve and measured by flowmeter 8.

The reactor is designed for the following flows: the primary gas flow mixture of 0.1 mmol ClO_2/s + 5 mmol N_2/s, the secondary gas mixture of 0.1 mmol NO/s + 1 mmol N_2/s by injector # 1, the secondary gas mixture of 0.1 mmol NO/s + 1 mmol N_2/s by injector # 2, and the secondary gas mixture of 0.1 mmol HI/s + 1 mmol N_2/s by injector # 3.

A column generator of ClO_2 (2) forms 100 cm long tube of inner diameter of 70 mm filled with solid $NaClO_2$. Gaseous ClO_2 is produced by reaction (2-14) realized by Cl_2 (diluted with N_2 (1:100)) through the column reactor. A total pressure in the reactor is about 100 kPa that the safety conditions of $P_{ClO2} \leq 4$ kPa (30 Torr) are fulfilled.

To be able to measure directly the ground state iodine atom concentrations in gas exiting the reactor, a continuous tunable single-mode 1.315 μm diode probe laser diagnostics will be used for monitoring the $I(^2P_{3/2}) - I(^2P_{1/2})$ absorption as soon as it is available from Samara (the instrument lent from the AFRL). Currently, the I atoms concentration is evaluated from determined concentrations of molecular iodine arising from the recombination of generated I atoms in the diagnostics cell 9 of ∅ 40 mm in which the gas velocity is 4 m/s only (comparing to 100 m/s in the flow reactor). The first detection place is very close to the

reactor exit, and the second detection place is 50 cm downflow. The absorption photometry at 488 nm is used by employing the Argon ion laser 10 equipped with the beam splitter 11. The concentration of generated I atoms is then evaluated from the rate constant of termolecular recombination of I atoms ($I + I + M \rightarrow I_2 + M$, $k = 4.2 \times 10^{-33}$ cm^6 s^{-1}) and measured I_2 concentration.

Gas exiting from the diagnostic cell passes a scrubber with solid bed of potassium hydroxide and liquid nitrogen trap (to remove I_2, HCl, residual HI, and partially also nitrogen oxides) and is exhausted by a rotary pump (25 m^3/h).

2.1.4. Experimental investigation and solved tasks

- The optimum number and radius of orifices in injectors of the flow tube reactor and diaphragm orifices in flowmeters were estimated (presented in details in Report 0002 of this Contract).

- Some suitable method of I atom detection was searched (a detailed literature review performed and the availability estimated).

- A dual optical detection system of I_2 for evaluation of I atoms concentration was designed, developed and tested.

- A calibration of diaphragm flowmeters was performed and their operation and all subsystems tested.

- A design and development of generator for ClO_2 production and its testing for different flowrate of Cl_2+N_2 mixture was performed including the analysis of the gas effluents. The results of this investigation are in **Tab. 8**.

Tab. 8

n_{Cl2}, μmol/s	35.5	40	52	70
n_{ClO2}, μmol/s	56.1	62	81	103
Y_{ClO2}, %	**78.9**	**77.3**	**78**	**73.5**

- A synthesis of some amount of gaseous HI was performed in collaboration with the Institute of Inorganic Chemistry to span a delay in delivering the HI from Matheson Co. in the USA (the only known producer of this chemicals). Two procedures were used. One method is based on dehydration of HI solution (67 % wt.) by either P_2O_5 or anhydrous $CaCl_2$, then drying of the produced gas, removing a residual water by trapping at -30° C, and liquefying of HI at -50° C. The liquid HI was transferred into a stainless steel gas bottle. The second method is based on the reaction of solid iodine with red phosphorus

$$2\,P + 5\,I_2 \rightarrow 2\,PI_5 \qquad (2\text{-}23)$$

and by hydrolysis of the formed iodide

$$PI_5 + 3\,H_2O \rightarrow HPO_3 + 5\,HI \qquad (2\text{-}24)$$

The produced gas is dried, liquefied, and bottled as given above.

- A data acquisition system by PC on-line using a special software was designed, developed and tested. The following parameters are recorded up to date: gas temperature measured by thermocouple just downstream the flow reactor, pressure in the diagnostic cell at the first optical detection place, pressures before diaphragms of three flow meters (6 - 8 in Fig. 15), and two amplified signals from silicon light detectors.

- **The first experiments with successful generation of I atoms were performed.**

2.2. Preliminary results of I atoms generation

The results of two first most successful experiments performed recently on atomic iodine generation are presented.

The flow conditions in experiment No. 1: primary flow: 58 μmol ClO_2/s
1st injector: 162 μmol NO/s
2nd injector: 168 μmol NO/s
3rd injector: 101 μmol HI/s

•

Fig. 16 shows the time course of flow rate of reactants and products, respectively. Contrary to the results following from the modeling, a relatively low temperature of the gas mixture was measured (500 K versus 320 K) which points out that produced HCl is mostly in the excited form.

The flow conditions in experiment No. 2: primary flow: 58 μmol ClO_2/s
1st injector: 110 μmol NO/s
2nd injector: 110 μmol NO/s
3rd injector: 95 μmol HI/s

- **The I atoms generation resulted in the flow rate of ~ 30 - 60 μmol I atoms/s. It corresponds to the I yield of 50 - 100% related to the ClO_2 flow rate, and 30 - 60 % related to the HI flow rate.**

During this experiment, however, some drift of the baseline of optical detectors was observed, which is the reason for some spread of values of I atoms flowrate.

2.3. Conclusion from the investigation

- The method of I atoms generation for a COIL was proposed, based on reaction of gaseous hydrogen iodide with atomic fluorine or chlorine.

- The 1-D model of both reaction systems was constructed and numerically solved with the result that the path via Cl atoms matches better to experimental conditions of the subsonic flow region of supersonic COIL.

- The small-scale device for atomic iodine generation was designed and constructed for the experimental verification of the results obtained by modeling.

- Many partial theoretical and experimental tasks were solved during the experimental work of I atoms generation.

- **The preliminary results show that the atomic iodine generation by suggested purely chemical method using gaseous reactants is possible and very promising for utilization in a COIL. The yields of I atom were very high exceeding 52 % related to the ClO_2 flow rate and 32 % related to the HI flow rate.**

3. References

1. J.E. Scott, J.L.R. Shaw, K.A. Truesdell, G.D. Hager, C.A. Helms, *AIAA paper*, 94-2436, 1994.
2. A. Pilař *et al.*, Příklady chemicko inženýrských výpočtů (in Czech) (Chemical Engineering Calculations, I/2, p. 22, SNTL 1962, Praha.
3. A.H. Shapiro, *The Dynamics and Thermodynamics of Compressible Fluids Flow*, 1953,Vol. I, p. 82.
4. L. Horwath, Modern Development in Fluid Dynamics High Speed Flow (in Russian) Vol. II, 1956.
5. K.M. Gruenewald, J. Handke, W.O. Shall, L.v.Entress-Fursteneck, *Proc. SPIE* Vol. **3574,** 315 (1998).
6. T.L. Rittenhouse, S.P. Phipps, Ch.A. Helms, *IEEE J. Quant. Electronics* **35**, 857 (1999).

4. Acknowledgement

The investigators are very grateful for the support of this work by the USAF European Office for Research and Development (EOARD). We thank very much to Prof. Martin Stickley, the Chief of Lasers, Optics and Materials, at the EOARD for his assistance with this contract.

We benefit very much during the work on the contract from discussions with Dr. Gordon Hager, Dr. Charles Helms and Dr. Harro Ackermann, and other workers from the US AFRL at the Kirtlend Base, NM.

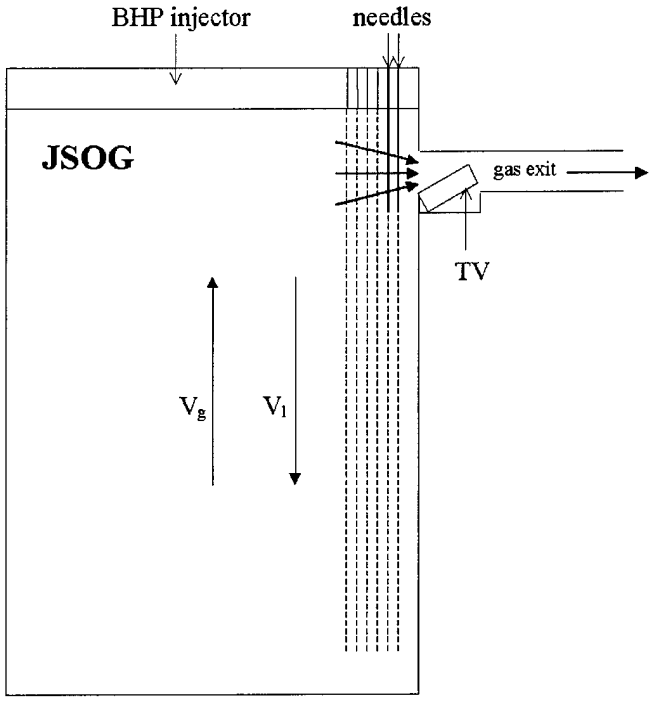
BHP injector
needles
JSOG
gas exit
TV
V_g
V_l

(a)

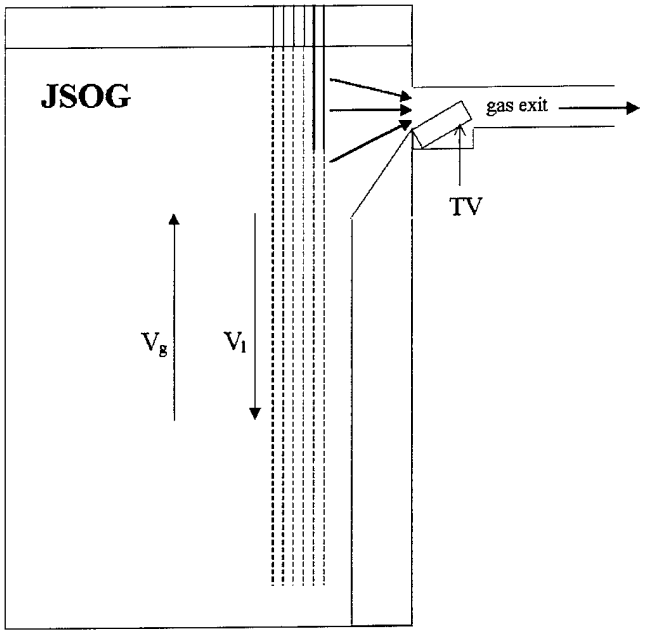
JSOG
gas exit
TV
V_g
V_l

(b)

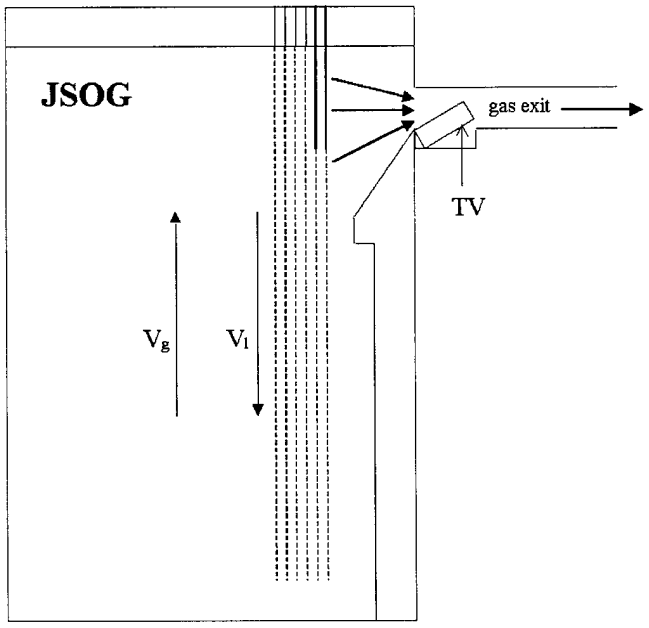
JSOG
gas exit
TV
V_g
V_l

(c)

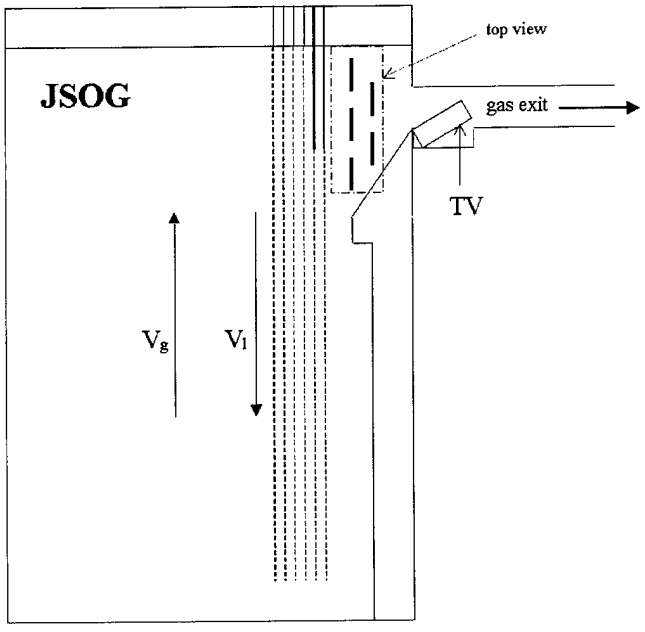
top view
JSOG
gas exit
TV
V_g
V_l

(d)

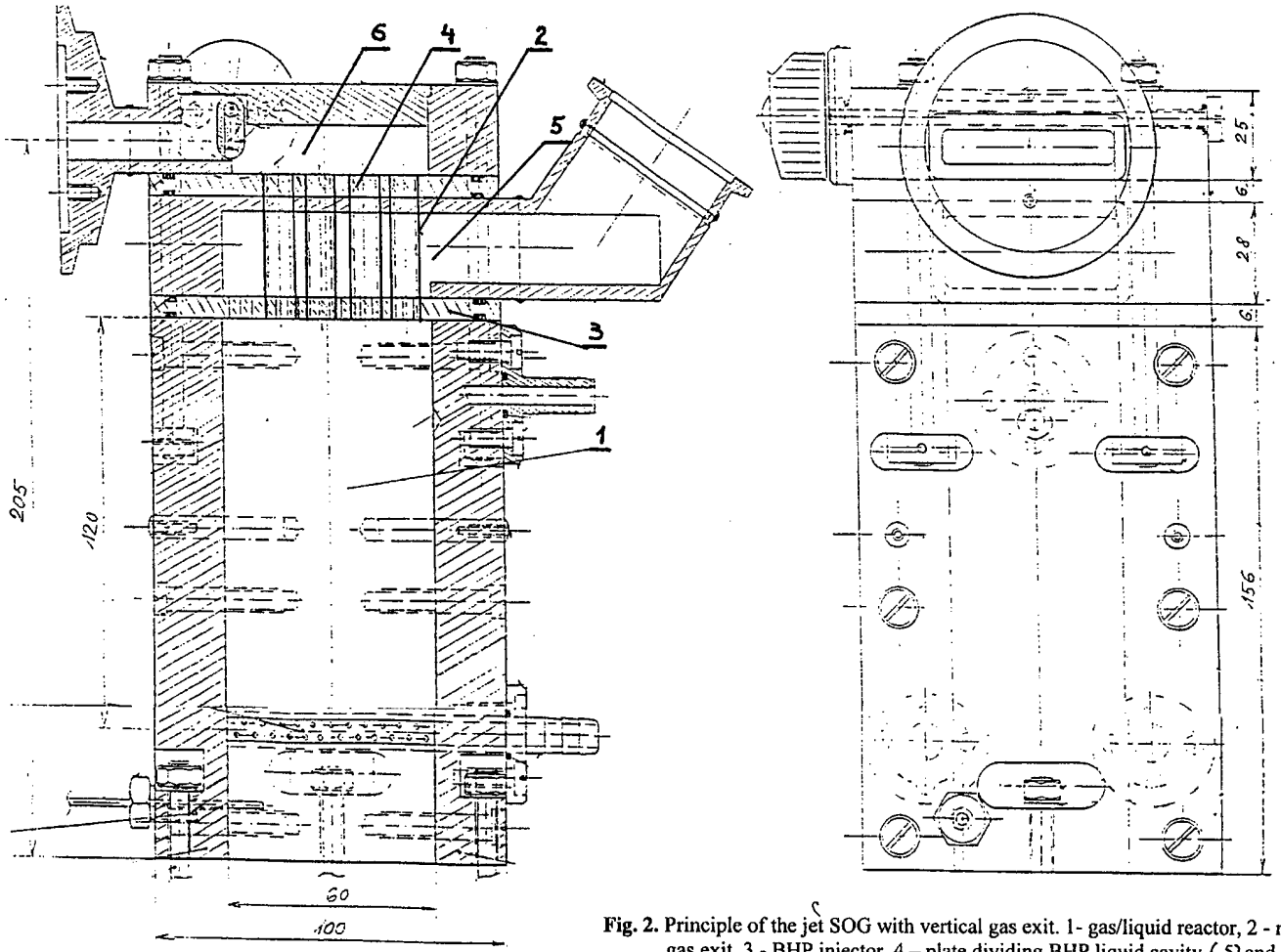

Fig. 2. Principle of the jet SOG with vertical gas exit. 1- gas/liquid reactor, 2 - metal tube gas exit, 3 - BHP injector, 4 – plate dividing BHP liquid cavity (5) and upper gas cavity (6).

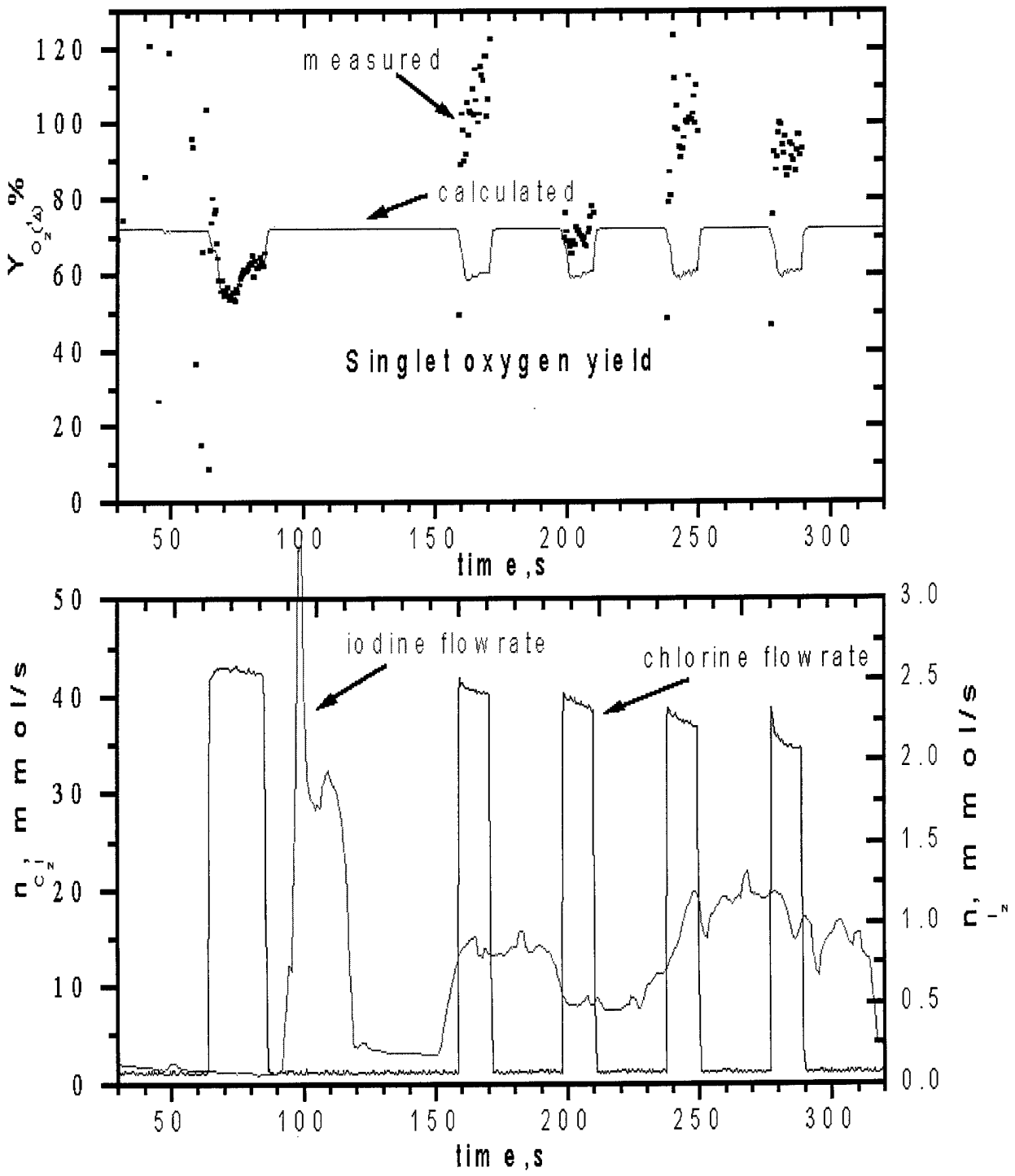

Fig.3. Measured and calculated singlet oxygen yield during interferring 1.27 nm signal with 1.315 nm signal from iodine

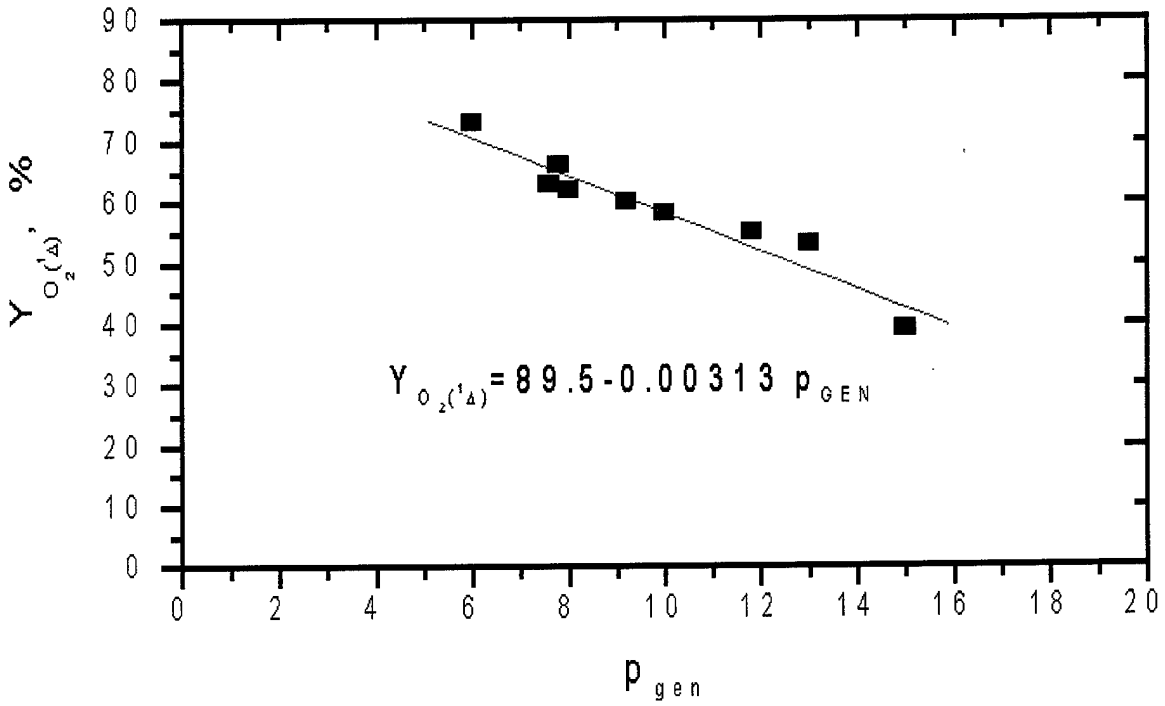

Fig.4. Yield of singlet oxygen as a function of generator pressure measured in the jet SOG with vertical gas exit (40 mmol Cl_2/s and 80 mmol He_{pr}/s)

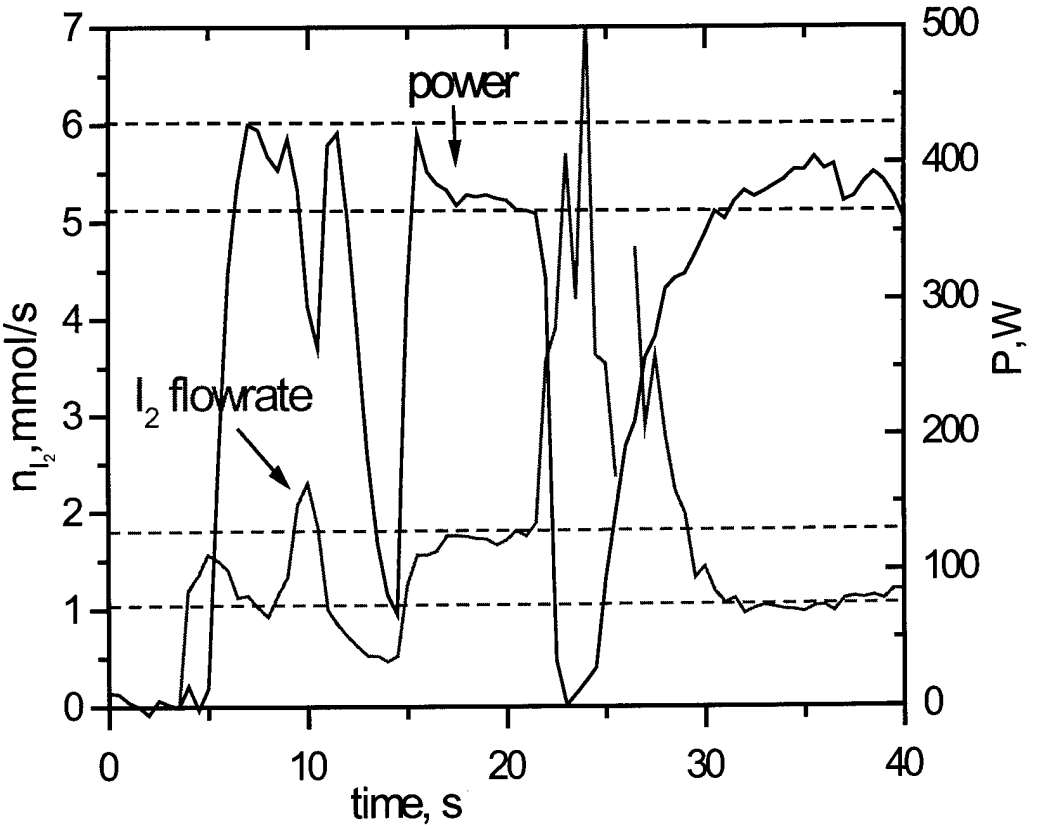

Fig.5. Simultaneous time course of laser power and I_2 flowrate

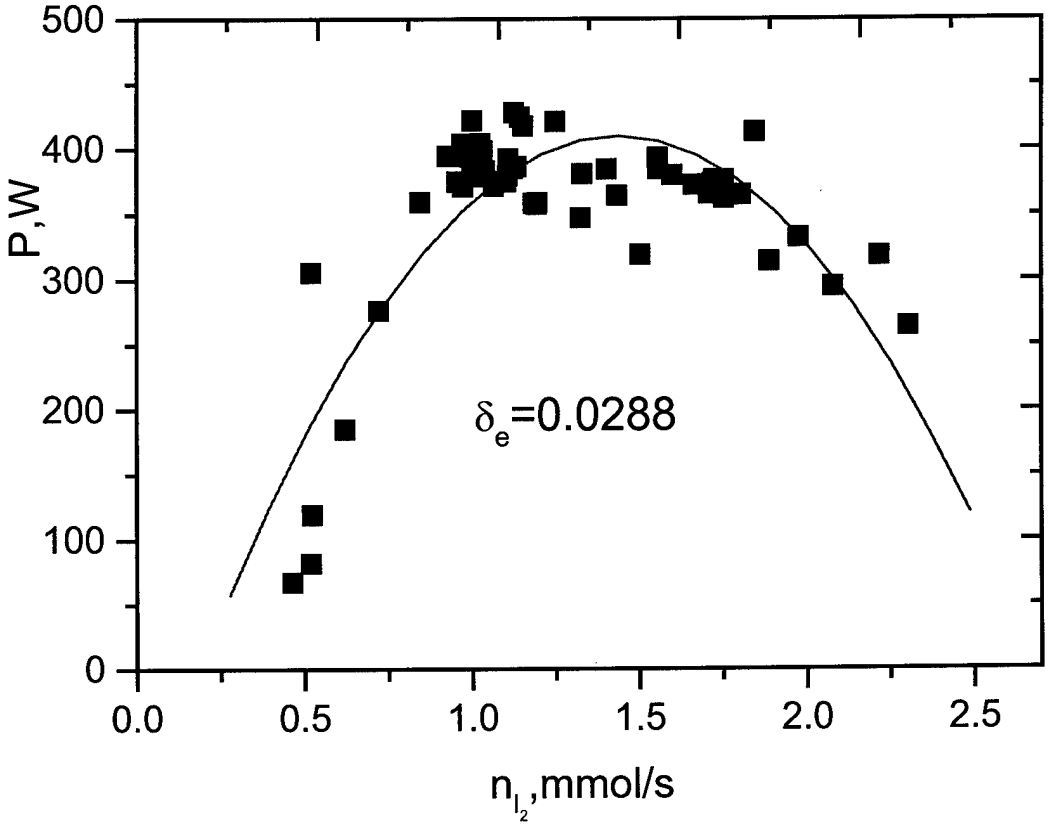

Fig.6. Laser power on iodine flowrate

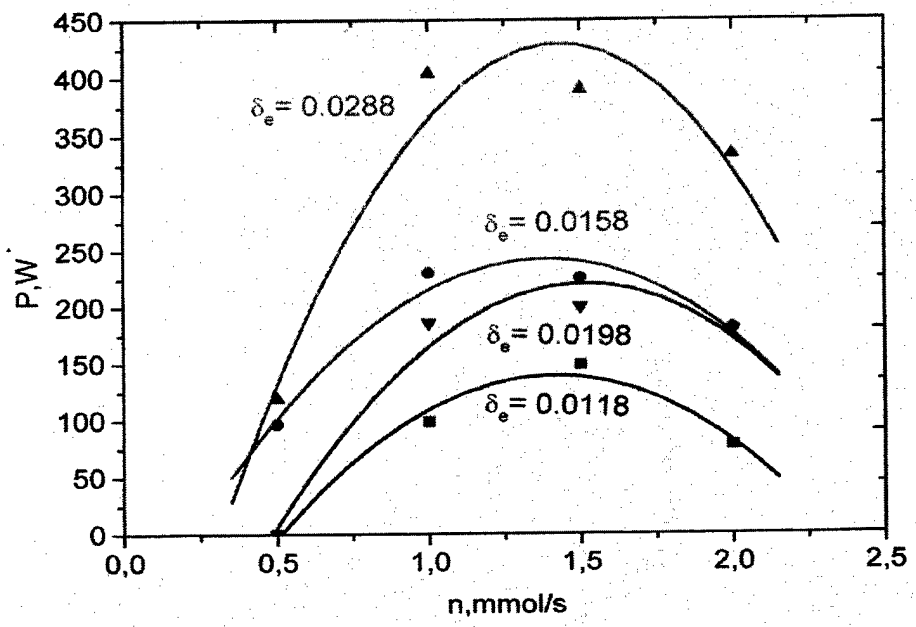

Fig.7. Laser power on iodine flowrate for different outcoupling

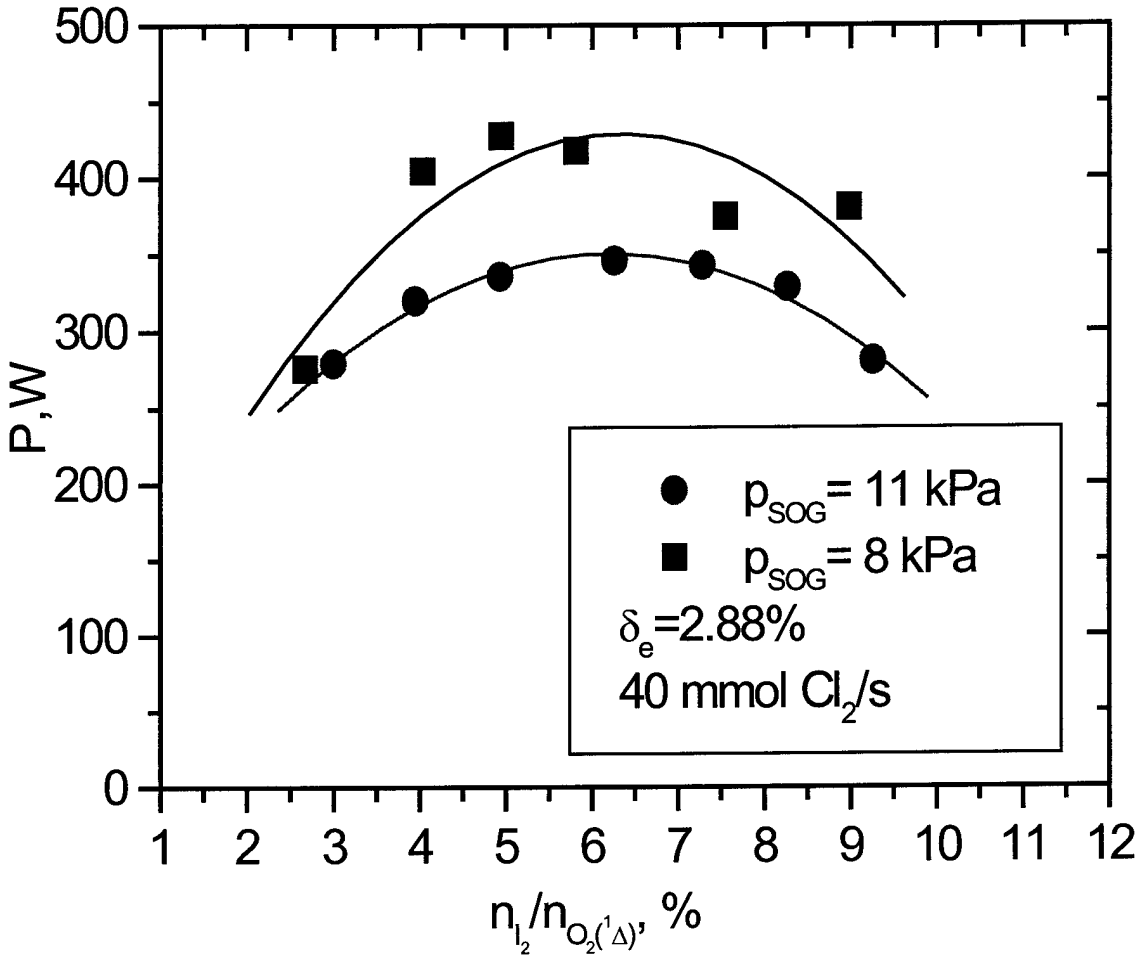

Fig.8. Output power in dependence on iodine to singlet oxygen ratio

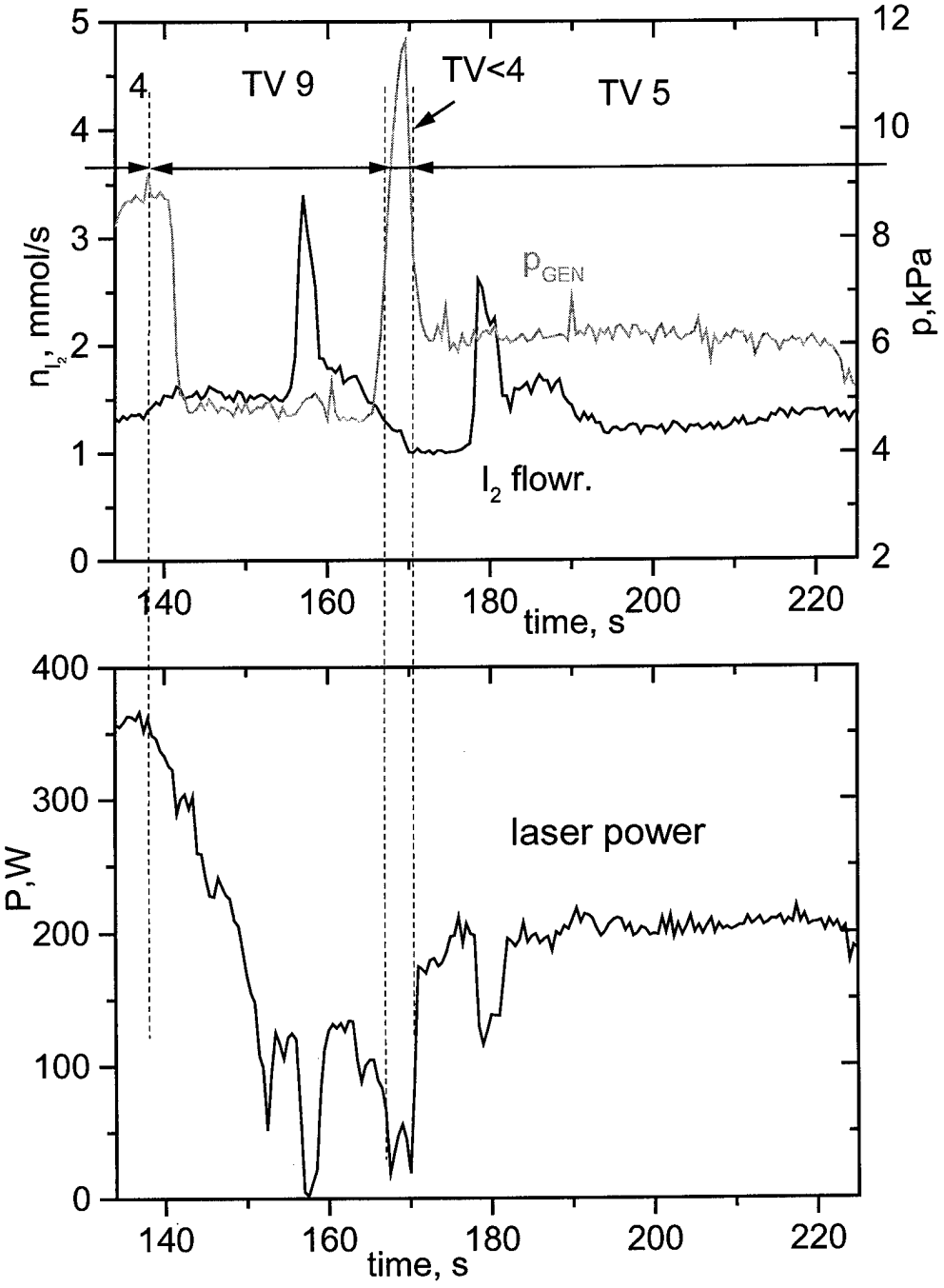

Fig.9: Time course of generator pressure, I_2 flowrate and laser power

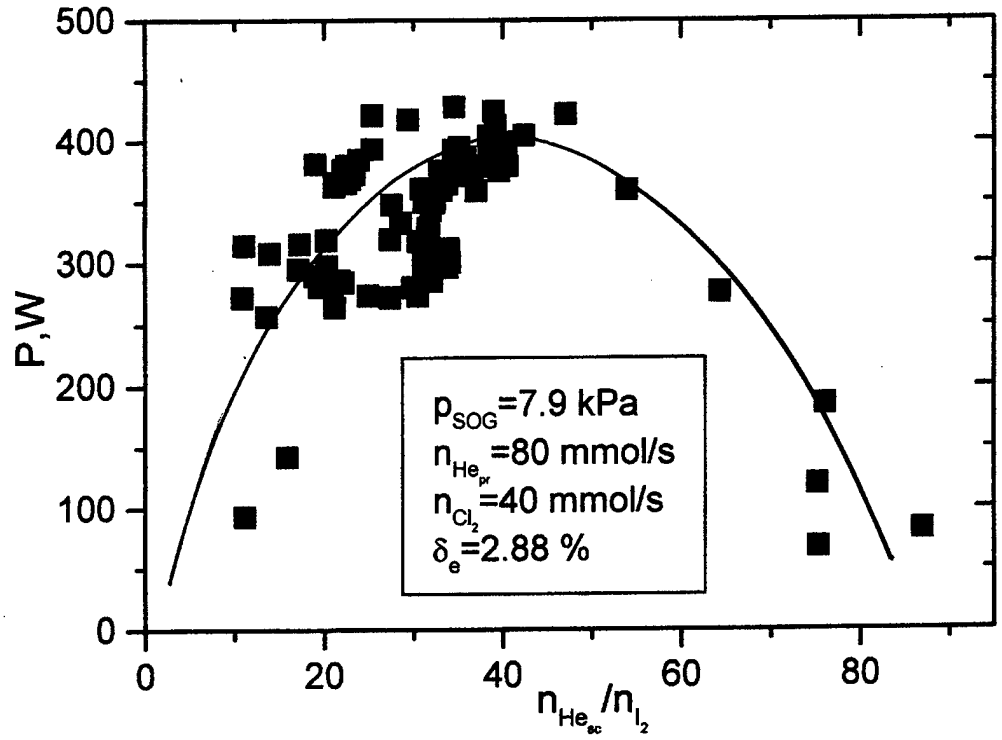
P,W
$n_{He_{sc}}/n_{I_2}$
p_{SOG}=7.9 kPa
$n_{He_{pr}}$=80 mmol/s
n_{Cl_2}=40 mmol/s
δ_e=2.88 %

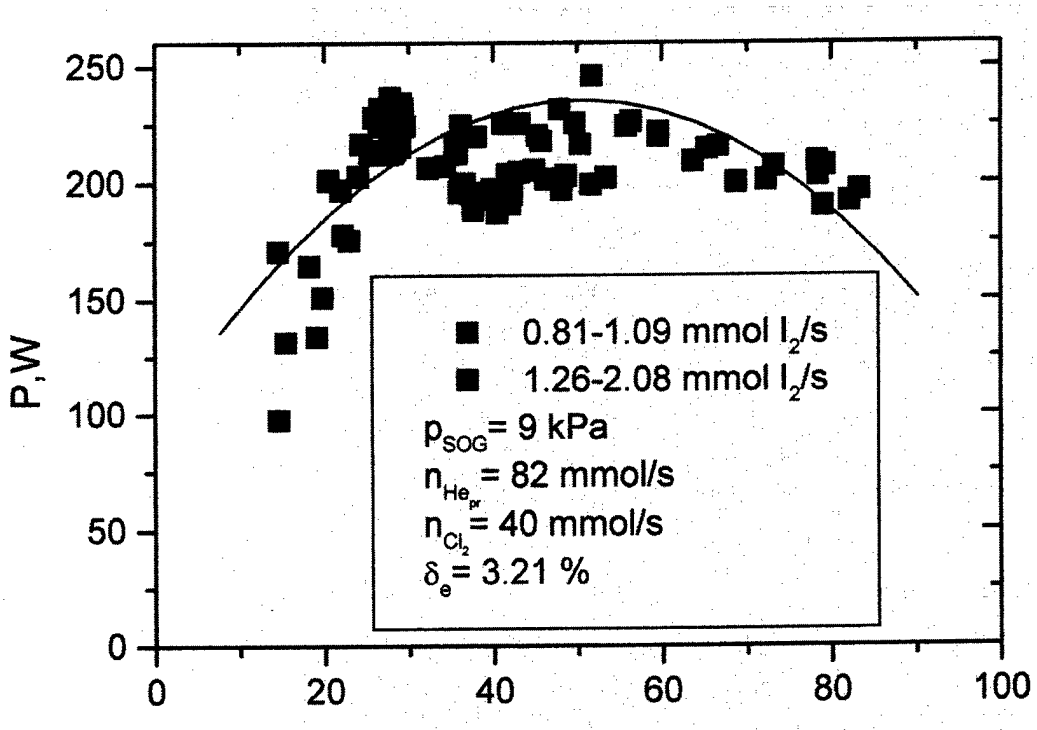
P,W
0.81-1.09 mmol I_2/s
1.26-2.08 mmol I_2/s
p_{SOG}= 9 kPa
$n_{He_{pr}}$ = 82 mmol/s
n_{Cl_2} = 40 mmol/s
δ_e = 3.21 %

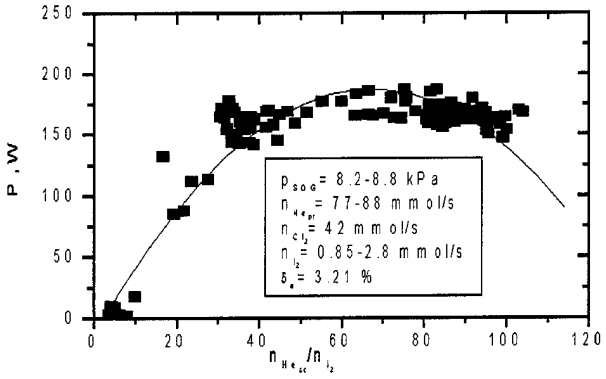

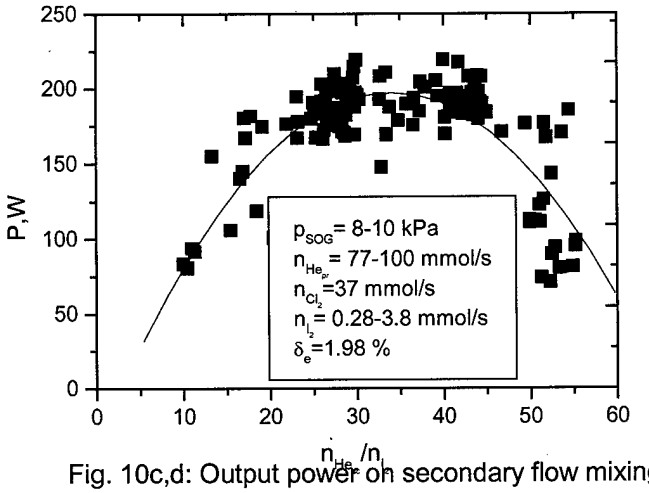

Fig. 10c,d: Output power on secondary flow mixing

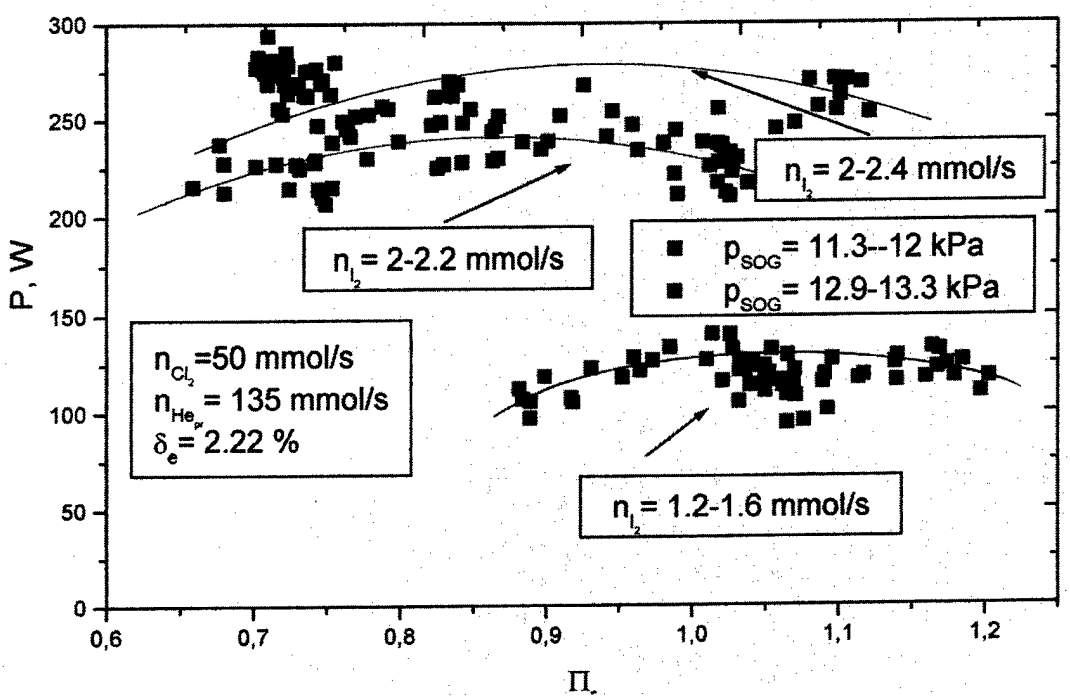
P, W
300
250
200
150
100
50
0
0,6
0,7
0,8
0,9
1,0
1,1
1,2
Π_r
n_{I_2} = 2-2.4 mmol/s
n_{I_2} = 2-2.2 mmol/s
p_{SOG}= 11.3--12 kPa
p_{SOG}= 12.9-13.3 kPa
n_{Cl_2}=50 mmol/s
$n_{He_{pr}}$ = 135 mmol/s
δ_e= 2.22 %
n_{I_2}= 1.2-1.6 mmol/s

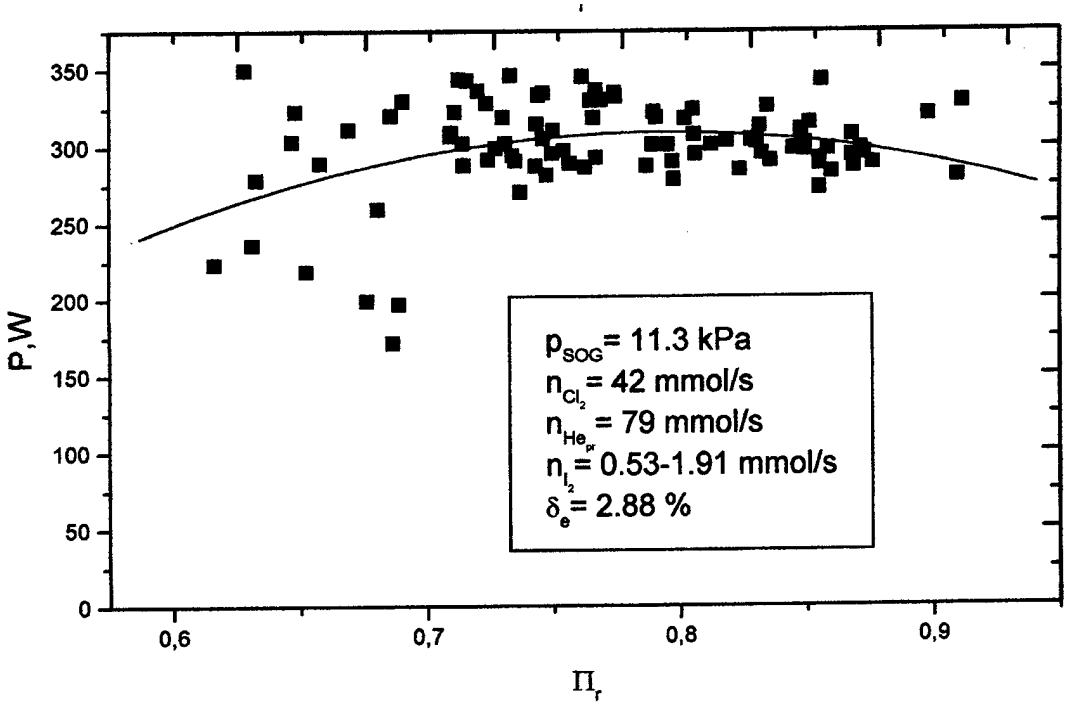
P,W
350
300
250
200
150
100
50
0
0,6
0,7
0,8
0,9
Π_r
p_{SOG}= 11.3 kPa
n_{Cl_2}= 42 mmol/s
$n_{He_{pr}}$ = 79 mmol/s
n_{I_2}= 0.53-1.91 mmol/s
δ_e= 2.88 %

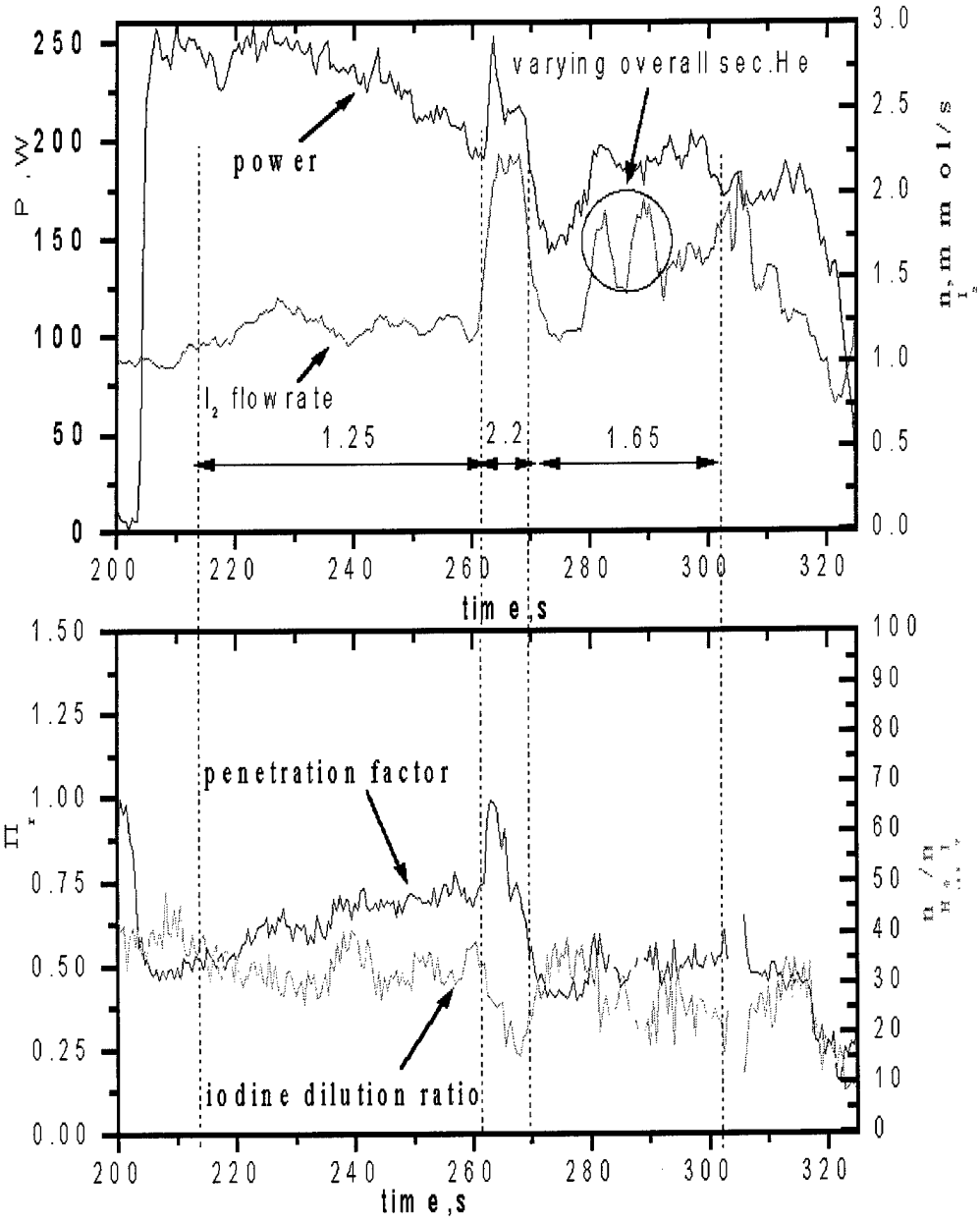

Fig.12a. Laser power as a function of changing iodine flowrate during one experimental run and relative penetration factor evaluated for a variable iodine dilution ratio

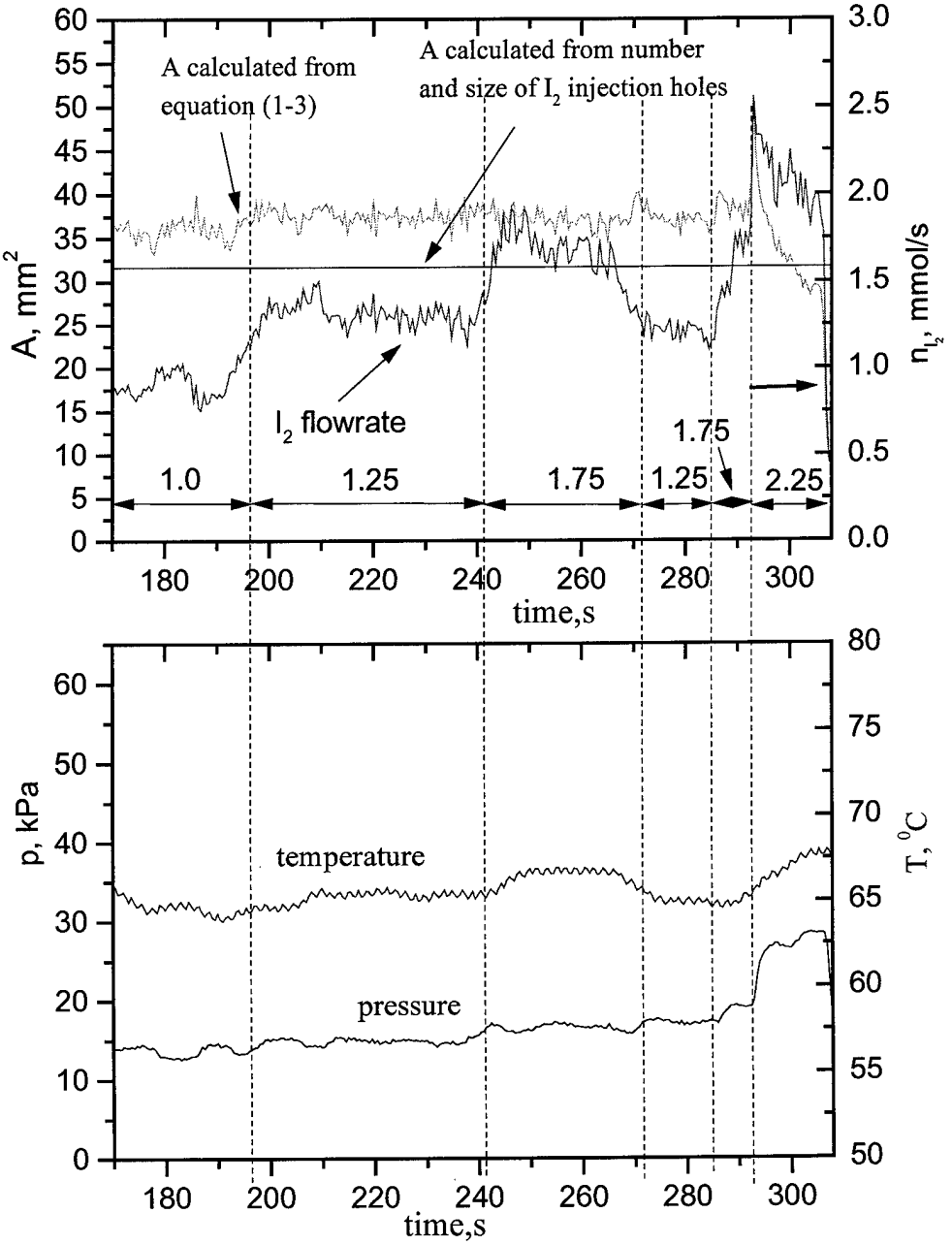

Fig.12b. Estimation of blocking the I_2 injector holes by evaluation of overall holes cross-section for various I_2 flowrate during one experimental run; corresponding I_2 vapor pressure and temperature in I_2 diagnostic cell

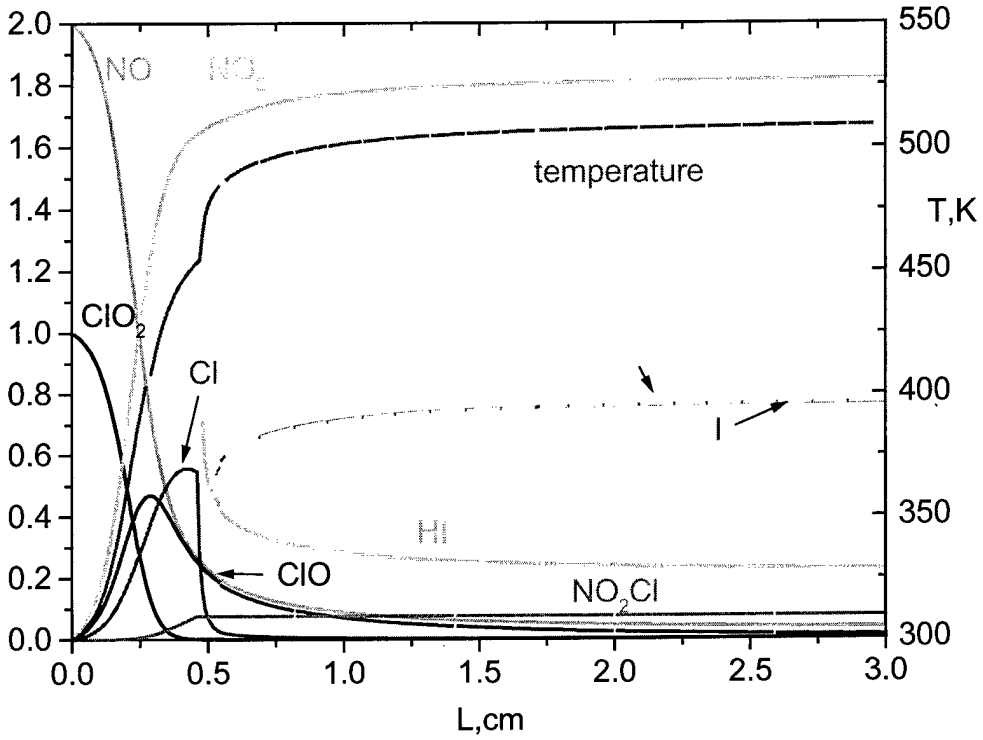

Fig.14. Atomic iodine generation via reaction of Cl with HI
$[ClO_2] : [NO] : [HI] : [He] = 1 : 2 : 1 : 75$, HI injected at $[Cl]_{max}$

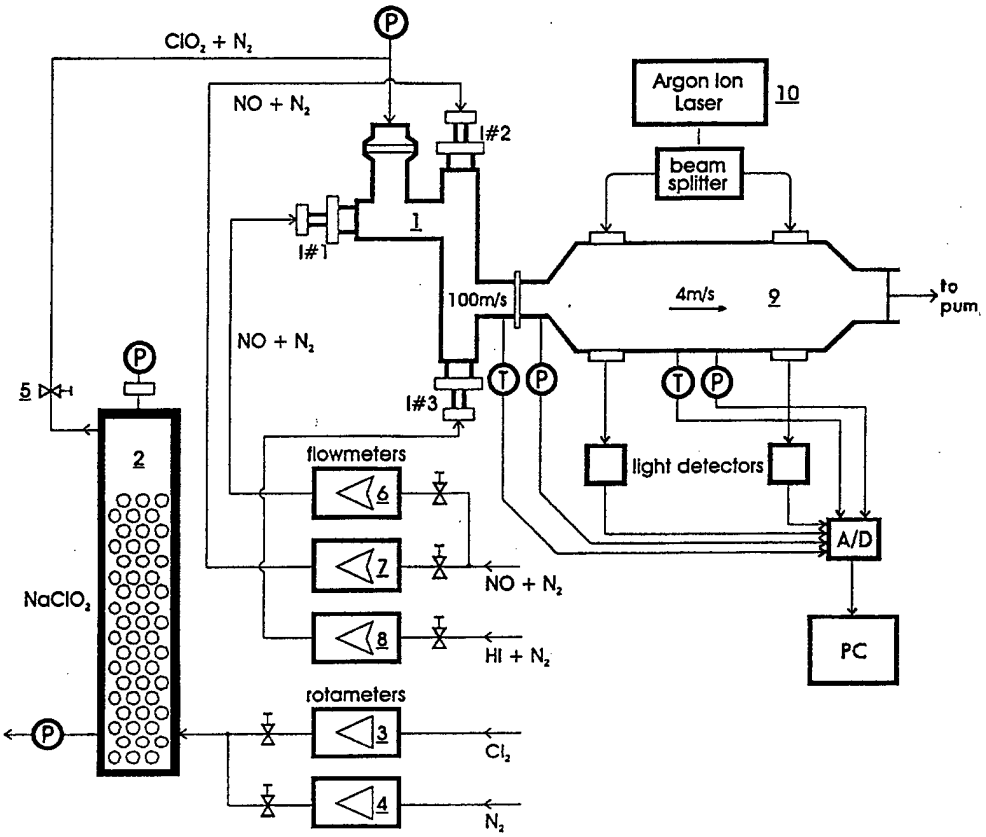

Fig. 15 Scheme of a small-scale device for atomic iodine generation

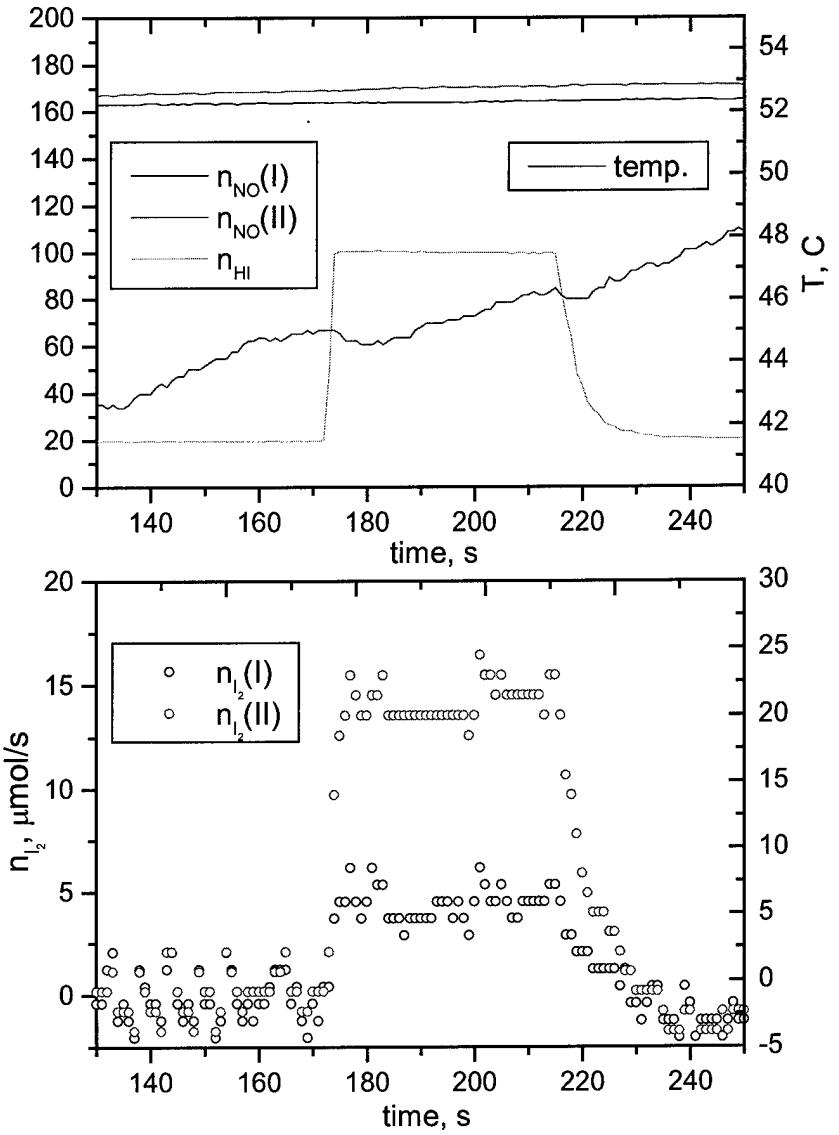

Fig. 16. Time course of flowrate of reactants and mixture temperature; flowrate of molecular iodine produced by recombination of atomic iodine measured at two detection places